SEMI - ANNUAL STATUS REPORT

(Period Covered: August 1, 1982 - January 31, 1983)

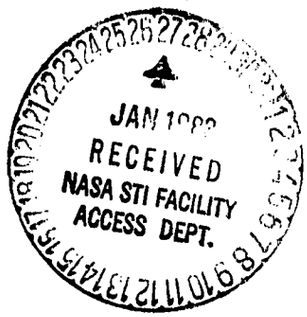

A COMPREHENSIVE MODEL TO DETERMINE THE EFFECTS OF TEMPERATURE AND SPECIES FLUCTUATIONS ON REACTION RATES IN TURBULENT REACTING FLOWS *

D. Goldstein, F. Magnotti and W. Chinitz **
The Cooper Union Research Foundation, Inc.
New York, New York 10003

* Work supported under Grant No. NAG1 - 18, National Aeronautics and Space Administration, Langley Research Center, High-Speed Aerodynamics Division, Hypersonic Propulsion Branch, Hampton, VA 23665

** Principal Investigator

TABLE OF CONTENTS

SUMMARY

The status of three tasks related to reaction rates in turbulent, reacting flows are reviewed. The work dealing with assumed - pdf modeling of reaction rates is currently investigating a three-variable pdf employing a "most-likely pdf" model. Studies related to appropriate chemical kinetic mechanisms treating hydrogen-air combustion have been initiated; their current status is reviewed. Perfectly-stirred reactor modeling of flame-stabilizing recirculation regions was used to investigate the stable flame regions for silane, hydrogen, methane and propane, and for certain mixtures thereof. It is concluded that in general, silane can be counted upon to stabilize flames only when the overall fuel-air equivalence ratio is close to or greater than unity. For lean flames, silane may tend to destabilize the flame. Other factors favoring stable flames are high initial reactant temperature and system pressure.

EFFECTS OF TEMPERATURE AND SPECIES FLUCTUATIONS ON REACTION RATES IN TURBULENT, REACTING FLOWS

1. Introduction

1.1 Overview

The prediction of turbulent reacting flows is a major concern of current combustion research. Such modeling is required in order to enhance the understanding of the phenomena involved and to design and evaluate the performance of combustion devices. A principle element to be derived from the modeling of these flows is an expression for the reaction rates of the various species involved in any particular combustion process under consideration.

Currently, several approaches for the determination of the properties of turbulent, reacting flows exist. [1] Of the present approaches, the method of utilizing an assumed probability density function (pdf) for temperature and species concentrations is selected for use in this study. The motivation for selecting this approach is its relative computational simplicity and basis in the probabilistic nature of turbulence.

1.2 Objective

This work examines the effects of temperature and species concentration fluctuations on reaction rates in turbulent reacting flows by means of the assumed pdf approach. The following items are the subject of the present study:

1. The most-likely joint pdf of reference [2] to describe effects of temperature and species concentration fluctuations on the reaction rate.

2. The extension of the most-likely joint pdf of reference [2] to three variables. This pdf is also used to describe temperature and species concentration fluctuations on the reaction rate.

Section 2 presents the general theory of pdf's and their use in calculating the mean turbulent reaction rate constant. Section 4 presents the results of these calculations. Section 5 presents the conclusions and direction for further study.

2. General Theory

2.1 Continuous Random Variables and Probability Density Functions

A variable x may be thought of as a continuous random variable if it can assume all values in some interval, where the endpoints of the interval may be plus and minus infinity. In a rigorous mathematical sense, x is said to be a continuous random variable if there exists a function p(x), which satisfies the following conditions: [3]

$$p(x) \geq 0$$
$$\int_{-\infty}^{\infty} p(x)\,dx = 1 \qquad (1)$$

It should be noted that p(x) by itself does not represent a probability, but rather the area under the curve from a to b represents the probability that the continuous random variable x will have a value somewhere on the interval. Thus the interpretation of equation (1b) is that the probability that x has a value somewhere over the entire range of values is unity. If the pdf is defined on a finite closed interval, [a,b], the probability of x having a value outside this interval must of course be zero.

The expected, or mean value, of a continuous random variable x is defined as: [3]

$$\mu_x = E(x) \equiv \int_{-\infty}^{\infty} x\,p(x)\,dx \qquad (2)$$

The variance of this same variable is defined as: [3]

$$\sigma_x^2 = V(x) = \int_{-\infty}^{\infty} (x - E(x))^2 \, p(x) \, dx \qquad (3)$$

The square root of the variance is the standard deviation.

The concept of the mean value of a continuous random variable can be extended to functions of a continuous random variable. For example, let h(x) be such a function. Then, the mean value of h(x) is: [3]

$$\overline{h(x)} = \int_{-\infty}^{\infty} h(x) \, p(x) \, dx \qquad (4)$$

Probability density functions can be defined for more than one continuous random variable. These are sometimes termed joint, multivariable or multi-dimensional pdf's. For a joint pdf of two continuous random variables, the probability is represented by the volume under the surface described by the pdf. For such a pdf, p(x,y), the conditions corresponding to equation (1) are:

$$\begin{aligned} & p(x,y) \geq 0 \\ & \int_{-\infty}^{\infty} \int_{-\infty}^{\infty} p(x,y) \, dxdy = 1 \end{aligned} \qquad (5)$$

The concepts of "moments" of a one-dimensional continuous random variable may be extended to multi-dimensional continuous random variables. For example, the joint moment about the origin of a two-dimensional continuous random variable, (x,y), is expressed as: [3]

$$\mu_{xy} = \int_{-\infty}^{\infty} \int_{-\infty}^{\infty} xy \, p(x,y) \, dxdy \qquad (6)$$

By comparison, equation (6) is seen to be an extension of equation (2).

The joint moment about the mean of a two-dimensional continuous random variable, (x,y), is expressed as: [3]

$$\mu_{xy} = \int_{-\infty}^{\infty}\int_{-\infty}^{\infty} (x - E(x))\,(y - E(y))\; p(x,y)\,dxdy \qquad (7)$$

μ_{xy} is also called the covariance of x and y.

By comparison, equation (7) is seen to be an extension of equation (3).

If a joint pdf is specified, it is possible to examine the distribution of any one of the continuous random variables by consideration of its marginal pdf. For a two-dimensional pdf, p(x,y), the marginal pdf of x, for example is given by: [3]

$$h(x) = \int_{-\infty}^{\infty} p(x,y)\,dy \qquad (8)$$

This marginal distribution of x may be thought of as the distribution of x, with the simultaneous behavior of the other variables suppressed. In other words, only the behavior of x is being examined.

Using the concept of a marginal pdf, the moment about the origin of any of the one-dimensional components of a multi-dimensional continuous random variable may be expressed. For a two-dimensional continuous random variable, the moment about the origin of x, for example, is given by:

$$\mu(x) = \int_{-\infty}^{\infty}\int_{-\infty}^{\infty} xp(x,y)\,dydx \qquad (9)$$

Examination of equations (8) and (9) reveals that the moment about the origin of x is expressed as the integral from $-\infty$ to $+\infty$, with respect to x, of the product

of x and its marginal pdf.

In the case of joint pdf's and functions of more than one continuous random variable, a similar expression to equation (4) can be written. For a function dependent of two continuous random variables, say g(x,y), the mean value is written as: [3]

$$\overline{g(x,y)} = \int_{-\infty}^{\infty}\int_{-\infty}^{\infty} g(x,y)\, p(x,y)\, dxdy \qquad (9)$$

The correlation coefficient, ρ_{xy}, is a parameter defined for the two-dimensional continuous random variable (x,y) as:

$$\rho_{xy} = \frac{E\{[x - E(x)][y - E(y)]\}}{V(x)\, V(y)} \qquad (10)$$

The numerator of the correlation coefficient is the covariance, shown in equation (7).

It is demonstrated in Reference [3] that the value of the correlation coefficient is always between -1 and +1.

If $\rho_{xy} = \pm 1$, x and y are linear function of each other. A negative value of ρ_{xy} indicates one variable increases while the other decreases. A positive value indicates that both variables increase or decrease simultaneously. A value of ρ close to zero only indicates the absence of a linear relationship between x and y. It does not preclude the possibility of some nonlinear relationship.

2.2 Arrhenius Reaction Rate Constant and Reaction Rate Expressions

For the purpose of this study, the following one-step, irreversible

reaction is considered:

$$F + \nu O \rightarrow P \tag{12}$$

F,O,P = fuel, oxidizer, and product species, respectively

ν = stoichiometric coefficient (molar)

The disappearance of F and O are related by:

$$\frac{-dC_F}{dt} = \frac{-1}{\nu}\frac{dC_O}{dt} \tag{13}$$

where: C_F , C_O = concentrations of fuel and oxidizer, respectively

The negative signs in equation (13) indicate that the concentrations of F and O decrease as the reaction proceeds. The reaction rate of fuel is expressed as:

$$\dot{w}_F = \frac{-dC_F}{dt} = k(T)C_F^{\,n}C_O^{\,m} \tag{14}$$

where k(T) = Arrhenius reaction rate constant
T = temperature
n,m = constants dependent upon the particular reaction

The Arrhenius reaction rate constant is expressed as:

$$k(T) = AT^B\exp(-T_A/T) \tag{15}$$

where A,B = constants dependent upon the particular reaction
T_A = activation temperature of the particular reaction

Equation (15) can be modified by the introduction of the dimensionless temperature:

$$t = \frac{T - T_{min}}{T_{max} - T_{min}} \tag{16}$$

The temperatures T_{max} and T_{min} are defined so that the dimensionless temperature t can only assume values within the interval [0,1]. Thus, T_{min} may be the lowest temerature of the unreacted constituents and T_{max} may be the equilibrium combustion temperature of the reaction. Substitution of (16) into (15) yields:

$$k(t) = A(k_1 t + k_2)^B \exp\left[-T_A/(k_1 t + k_2)\right] \tag{17}$$

where $k_1 = T_{max} - T_{min}$

$k_2 = T_{min}$

Equation (14) is also modified by the introduction of the following dimensionless concentrations:

$$r_F = \frac{C_F - C_F^{min}}{C_F^{max} - C_F^{min}} \; ; \; r_O = \frac{C_O - C_O^{min}}{C_O^{max} - C_O^{min}} \tag{18}$$

In these expressions, "max" and "min" denote maximum and minimum values, respectively. Equation (18) ensures that r_F and r_O only assume values within the interval (0,1). For the case where the minimum concentrations are zero and the maximum concentrations are the initial values, the combination of equations (14) and (18) yields:

$$\dot{w}_F = k(t)\,(r_F C_F^0)^n (r_O C_O^2)^m \tag{19}$$

where C_F^0, C_O^0 = initial concentrations of fuel and oxidizer, respectively

2.3 Mean Turbulent Arrhenius Reaction Rate Constant and Mean Turbulent Reaction Rate Expressions

In a turbulent reacting flow, the mean turbulent Arrhenius reaction rate constant can be calculated by treating the temperature as a continuous random variable and specifying an appropriate probability density function for the temperature. This concept is employed in Reference [4], along with the analogs of equations (4) and (17) in the present work, to yield:

$$\overline{k(t)} = {}_0\int^1 k(t)p(t)dt \tag{20}$$

where $\overline{k(t)}$ = mean turbulent Arrhenius reaction rate constant

The above expression provides a direct, relatively simple method of taking into account the effects of temperature fluctuations on the Arrhenius reaction rate constant in a turbulent, reacting flow.

Similarly, the expression for the mean turbulent reaction rate can be developed from an extension and combination of equations (10) and (19). Thus:

$$\overline{\dot{w}_F} = {}_0\int^1 {}_0\int^1 {}_0\int^1 \dot{w}_F p(t,r_F,r_O)\, dt\, dr_F\, dr_O \tag{21}$$

where $\overline{\dot{w}_F}$ = mean turbulent reaction rate of fuel

This expression utilizes a joint pdf for temperature and species. Equations (20) and (21) can be applied to one-step mechanisms or, multi-step mechanisms, by considering each elementary reaction separately. The pdf's used here are considered to be valid at an instant in time, and thus are not functions of time.

In order to compare the magnitude of a mean turbulent Arrhenius reaction rate constant to the corresponding laminar term, an "amplification ratio" is defined. The laminar Arrhenius reaction rate constant is calculated by inserting the mean dimensionless temperature in equation (17). The reaction rate constant amplification ratio is obtained by dividing equations (20) by (17):

$$Z = \overline{k}_t / k_1 \tag{22}$$

where Z = reaction rate constant amplification ratio

$\overline{k}_t$ = mean turbulent reaction rate constant

k_1 = corresponding laminar reaction rate constant

A similar term may be defined for the ratio of a mean turbulent reaction rate to the corresponding laminar reaction rate. The laminar reaction rate is calculated by inserting mean values of dimensionless temperature and concentrations into equation (19). The ratio of equation (21) and (19) defines the reaction rate amplification ratio:

$$Z' = \dot{\overline{w}}_t / \dot{w}_1 \tag{23}$$

where Z' = reaction rate amplification ratio

$\dot{\overline{w}}_t$ = mean turbulent reaction rate

$\dot{w}_1$ = corresponding laminar reaction rate

Equation (23) is the reaction rate amplification ratio in which the mean turbulent reaction rate is calculated with consideration of the combined effects of

temperature and species concentrations fluctuations. In order to compare this amplification ratio to one which considers only temperature fluctuations, the following is defined with the aid of equation (19):

$$Z = \frac{k_t(r_F C_F^{\circ})^n (r_O C_O^{\circ})^m}{k(\bar{r}_F C_F^{\circ})^n (\bar{r}_O C_O^{\circ})^m}$$

This expression involves a mean turbulent reaction rate in which a mean turbulent reaction rate constant is employed along with laminar values of concentrations. The corresponding laminar reaction rate also contains these same concentration terms. Thus, the concentration terms cancel. The reaction rate amplification ratio for this case is:

$$Z' = \bar{k}_t / k_l \tag{24}$$

This amplification ratio may be compared to that calculated by use of equation (23). Hence, combined effects of temperature and species concentrations fluctuations on the reaction rate may be compared to effects of only temperature fluctuations.

3. Joint Probability Density Functions For Temperature & Species

3.1 Most-Likely Bivariate pdf for Two Species

A model which accounts for the combined effects of temperature fluctuations and concentrations fluctuations of both fuel and oxidizer species, explicitly, on the mean turbulent reaction rate is presented in this section. As an initial step in the formulation of such a model, temperature is treated as an independent random variable, and as such, has no effect on the species concentrations.

Mathematically, the three-variable pdf for temperature and species is expressed as:

$$p(t,r_F,r_O) = f(t)g(r_F,r_O), \qquad \begin{aligned} 0 \le t &\le 1 \\ 0 \le r_F &\le 1 \\ 0 \le r_O &\le 1 \end{aligned} \tag{25}$$

where $f(t)$ = a pdf for temperature
$g(r_F,r_O)$ = a joint pdf for the concentrations of fuel and oxidizer species

for the case where temperature is treated as an independent continuous random variable. Equation (25) is a valid pdf since it satisfies the following extension of equations (5a) and (5b) for a three-variable pdf:

$$p(t,r_F,r_O) \ge 0 \tag{26a}$$

$$\int_0^1 \int_0^1 \int_0^1 p(t,r_F,r_O)\,dt\,dr_F\,dr_O = 1 \tag{26b}$$

The most-likely bivariate pdf is used as the joint pdf for the concentrations of fuel and oxidizer species in this model. The most likely bivariate pdf of Reference [4] can be written in the generalized form:

$$P_\lambda(\psi) = q(\psi) \exp\left(\sum_{n=0}^{\lambda} A_n \psi^n\right) \tag{27}$$

where $q(\psi)$ is the a priori probability which, for non-reactive scalars, is a constant. The $(\lambda+1)$ coefficients A_λ are uniquely determined from the moments and from the condition that the pdf integrates to unity. When the first three moments are known for the pdf, it shows excellent agreement with experimental data.

As an initial step in the utilization of the most-likely bivariate pdf for two species, a pdf based on the first moment about the origin of each species concentration and the covariance of the two concentrations is selected. The expression for the chosen form of the most-likely bivariate pdf for two species is:

$$g(r_F, r_O) = q \cdot \exp(\lambda_O + \lambda_1 r_F + \lambda_2 r_O + \lambda_3 r_F r_O) \tag{28}$$

where q = a constant

r_F = dimensionless concentration of the fuel

r_O = dimensionless concentration of oxidizer

The continuous random variables in equation (28) are treated as passive scalars.

With this simplification, the "q" term in equation (28) is a constant. The value of this constant "q" term is shown in Appendix A of Ref. 2 to have no effect on the calculated value of the most-likely bivariate pdf and the values of the resulting reaction rates.

The values of the constant coefficeints, $\lambda_0, \lambda_1, \lambda_2, \lambda_3$, in equation (28) are obtained from the simultaneous solution of the following constraint equations for known values of $\bar{r}_F$, $\bar{r}_O$ and $\overline{r'_F r'_O}$:

$$\int_0^1 \int_0^1 g(r_F, r_O) dr_F \, dr_O = 1 \tag{29}$$

$$\int_0^1 \int_0^1 r_F \, g(r_F, r_O) dr_F \, dr_O = \bar{r}_F \tag{30}$$

$$\int_0^1 \int_0^1 r_O \, g(r_F, r_O) dr_F \, dr_O = \bar{r}_O \tag{31}$$

$$\int_0^1 \int_0^1 (r_F - \bar{r}_F)(r_O - \bar{r}_O) \, g(r_F, r_O) \, dr_F \, dr_O = \overline{r'_F r'_O} \tag{32}$$

The pdf selected for temperature is either the beta pdf, the one-variable most-likely pdf, as presented in reference [2] or the ramp pdf, based on certain criteria specified in Reference [5]. The development and utilization of these criteria are discussed in Reference [5] and will not be discussed here.

Equation (25) is used in an expression for the mean turbulent reaction rate by considering the one-step, irreversible reaction, as in Section 2.2:

$$F + \nu O \rightarrow P$$

where F,O,P = fuel, oxidizer and product species, respectively

ν = stoichiometric coefficient (molar)

Assuming that both n and m are equal to unity in equation (19), the reaction rate of the fuel may be written as:

$$\dot{w}_F = k(t)\,(r_F C_F^0)\,(r_O C_O^0) \tag{34}$$

For the case of statistical independence between temperature and species concentration, the expression for the mean turbulent reaction rate of the fuel species is obtained from a combination of equations (17), (21) and (25). This yields:

$$\overline{\dot{w}}_t = -A \int_0^1 (k_1 t+k_2)^B \exp\left[-T_A/(k_1 t+k_2)\right] f(t)\,dt \cdot C_F^0 C_O^0 \int_0^1 \int_0^1 r_F r_O\, g(r_F, r_O)\, dr_F\, dr_O \tag{35}$$

The corresponding value of the laminar reaction rate is determined by inserting the appropriate values of $\bar{t}$, $\bar{r}_F$ and $\bar{r}_O$ into the combination of equations (17) and (33). This yields:

$$\dot{w}_1 = -A\,(k_1\bar{t}+k_2)^B \exp\left[-T_A/(k_1\bar{t}+k_2)\right] \bar{r}_F C_F^0\ \bar{r}_O C_O^0 \tag{36}$$

The reaction rate amplification ratio is obtained by dividing equation (35) by (36). This yields:

$$Z' = \frac{\int_0^1 (k_1 t+k_2)^B \exp\left[-T_A/(k_1 t+k_2)\right] f(t)\,dt \cdot \int_0^1 \int_0^1 r_F r_O\, g(r_F, r_O)\, dr_F\, dr_O}{(k_1\bar{t}+k_2)^B \exp\left[-T_A/(k_1\bar{t}+k_2)\right]\ \bar{r}_F\ \bar{r}_O} \tag{37}$$

The amplification ratio in equation (37) may be expressed as the product of a term which accounts for the effects of temperature fluctuations, Z_t' , and a term which accounts for the effects of species concentrations fluctuations, Z_r' . These terms are expressed as follows:

$$Z_t' = \frac{{}_0\int^1 (k_1 t+k_2)^B \exp\left[-T_A/(k_1\bar{t}+k_2)\right] f(t)\, dt}{(k_1\bar{t}+k_2)^B \exp\left[-T_A/(k_1\bar{t}+k_2)\right]}$$

$$Z_r' = \frac{{}_0\int^1 {}_0\int^1 r_F r_O\, g(r_F, r_O)\, dr_F\, dr_O}{\bar{r}_F \bar{r}_O} \qquad (38)$$

Comparison of equations (38) and (22) illustrates that Z_t' is equal to Z.

In this study, values of dimensionless mean concentrations are varied over the range 0.0 to 1.0 , and the values of mean square fluctuations of dimensionless concentration are varied over the range 0.0 to 0.1 . The value of the correlation coefficient between the fuel and oxidizer is assumed to be -0.9 [1]. The covariance can then be determined from:

$$\overline{r_F' r_O'} = \rho \quad \bar{r}_F'^2 \quad \bar{r}_O'^2 \qquad (39)$$

where ρ = correlation coefficient
$\bar{r}'^2$ = mean square fluctuation

The computational procedure to determine Z_r' is described below:

1. Select values for $\bar{r}_F$, $\bar{r}_O$, $\bar{r}_F'^2$ and $\bar{r}_O'^2$.

2. Calculate the covariance, using equation (39) and a correlation coefficient of -0.9.

3. Use Newton's Method to solve for the constant coefficients of equation (28).

4. Integrate equation (38) to calculate Z_r'.

The entries to the augmented matrix for Newton's Method and the related mathematical limitations for the most-likely bivariate pdf will be described in the next status report. The data obtained from this parameter study are presented in their entirety in Reference [6]. Representative results are presented in Section 4.1. The results of this parameter study are being compared to experimental data, to judge the validity of this model and the assumptions on which it is based.

The model given by $Z = Z_t' \cdot Z_r'$ is currently being examined in a large-scale computer program at NASA Langley. The portion of the reaction rate amplification ratio which accounts for temperature fluctuations, is calculated from either the beta pdf or the ramp pdf. The selection criteria is specified in Reference [5]. Z_r', the portion of the reation rate amplification ratio which accounts for the effects of species concentration fluctuations is supplied in the form of a subroutine for the computer program.

Subroutine FINDZ is called to find the value of the unmixedness multiplier, Z_r -- given the mass fractions of species A and B and the corresponding fluctuations of the mass fractions.

The values of Z_r' are stored as elements of the matrix ABCD. For given values of RA, RB, RSA, and RS , find Z_r'. The problem is symmetric in values for RA and RB ; the same is true for values of RSA and RSE.

A finite number of values of Z_r' are stored in ABCD. These correspond to RA = 0, .1, .2, ...,1, RSB = 0., .01, .02, ..,.1.

The given values of RA, RB , RSA, and RSB are decimal figures with more than one significant figure. Therefore, interpolation is necessary. This is accomplished by finding the 16 values of Z_r' which are nearest neighbors to the desired value - one larger and one smaller. For each given value of RA, RB, RSA, and RSB, these sixteen values are added and the result is divided by sixteen.

3.2 An Alternative Three-Variable Model

A full three variable model for temperature and two species concentrations is discussed in this section. The assumption of statistical independence between temperature and species concentration has been dropped in this model. The assumed pdf for the full three-variable model uses a joint pdf for <u>both</u> the temperature and species concentrations, and is of the form:

$$p(t,r_F,r_O) = q \cdot \exp(\lambda_0+\lambda_1 t+\lambda_2 r_F+\lambda_3 r_O+\lambda_4 t r_F+\lambda_5 t r_O+\lambda_6 r_F r_O) \quad (40)$$

where q = a priori probability

$\lambda_O - \lambda_6$ = adjustable constants

This full three-variable model is an extension of the statistically "most-likely" bivariate pdf in Reference [4] as shown in equation (27), when all of the first and second moments are known for the pdf. The physical justification for using this pdf and extensions of it was previously discussed in Section 3.1.

The values of the constant coefficients, λ_0, λ_1, λ_2, λ_3, λ_4, λ_5, and λ_6, in equation (40) are obtained from the simultaneous solution of the following constraint equations for known values of $\bar{t}$, $\bar{r}_F$, $\bar{r}_O$, $\overline{r_F't'}$, $\overline{r_O't'}$, $\overline{r_F'r_O'}$:

$$\int_0^1\int_0^1\int_0^1 p(t, r_F, r_O)\, dt dr_F dr_O = 1 \tag{41}$$

$$\int_0^1\int_0^1\int_0^1 t\, p(t, r_F, r_O)\, dt dr_F dr_O = \bar{t} \tag{42}$$

$$\int_0^1\int_0^1\int_0^1 r\, p(t, r_F, r_O)\, dt dr_F dr_O = \bar{r}_F \tag{43}$$

$$\int_0^1\int_0^1\int_0^1 r_O\, p(t, r_F, r_O)\, dt dr_F dr_O = \bar{r}_O \tag{44}$$

$$\int_0^1\int_0^1\int_0^1 (t - \bar{t})\,(r_F - \bar{r}_F)\, p(t, r_F, r_O)\, dt dr_F dr_O = \overline{t'r_F'} \tag{45}$$

$$\int_0^1\int_0^1\int_0^1 (t - \bar{t})\,(r_O - \bar{r}_O)\, p(t, r_F, r_O)\, dt dr_F dr_O = \overline{t'r_O'} \tag{46}$$

$$\int_0^1\int_0^1\int_0^1 (r_F - \bar{r}_F)\,(r_O - \bar{r}_O)\, p(t, r_F, r_O)\, dt dr_F dr_O = \overline{r_F'r_O'} \tag{47}$$

The temperature and species concentration in equation (40) are treated as passive scalars. With this simplification, the "a priori" probability q is a constant. The proof shown in Ref. 2 can be extneded to show that the q term in equation (40) will not effect the calculated value of the pdf, $p(t, r_F, r_O)$, and therefore has no effect on the resulting reaction rate.

The pdf, $p(t,r_F,r_O)$, is used in an expression for the mean turbulent reaction rate by considering any irreversible reaction of the form:

$$A + B \rightarrow C + D \tag{48}$$

where A, B = reactants species

C, D = product species

Assuming that both n and m are equal to unity in equation (14), the reaction rate of the fuel may be written as:

$$\dot{w}_F = k(t)\,(r_F C_F^0)\,(r_O C_O^0) \tag{49}$$

A combination of equations (17), (21), and (25) yield an expression for the mean turbulent reaction rate as:

$$\dot{w}_t = -A\,C_F^0 C_O^0 \int_0^1 \int_0^1 \int_0^1 (k_1 t+k_2)^B \exp(-T_A/(k_1 t+k_2)) \cdot r_F r_O p(t,r_F,r_O)\,dt\,dr_F\,dr_O \tag{50}$$

The corresponding value of the laminar reaction rate is determined by inserting the appropriate values of $\bar{r}_F$, $\bar{r}_O$, and $\bar{t}$ into the combination of equations (17), and (33). This yields:

$$\dot{w}_l = -A(k,t+k_2)^B \exp\left(-T_A/(k,\bar{t}+k_2)\right) \bar{r}_F C_F^0 \bar{r}_O C_O^0 \tag{51}$$

The reaction rate amplification ratio is obtained by dividing equation (50) by (51), yielding:

$$Z = \frac{{}_0\int^1{}_0\int^1{}_0\int^1 r_F r_O (k_1 t+k_2)^B \exp[-T_A/(k_1 t+k_2)]\, p(t, r_F, r_O)\, dt\, dr_F\, dr_O}{\bar{r}_F \bar{r}_O (k_1 \bar{t}+k_2)^B \exp[-T_A/(k_1 \bar{t}+k_2)]} \qquad (52)$$

In this parameter study, the dimensionless mean temperature and the dimensionless mean concentrations are varied over the range from 0.1 to 0.9. The values of mean square fluctuations of dimensionless concentrations and mean square fluctuations of dimensionless temperature are varied over the range from 0.01 to 0.09. The corresponding value of the covariance for $\overline{r_F' r_O'}$ is determined from equation (39) using an assumed value of the correlation coefficient of -0.9[1]. The covariance for $\overline{r_F' t'}$ and $\overline{r_O' t'}$ are also calculated with a correlation coefficient of -0.9 for a similar form of equation (39).

The computational procedure to determine the values of the reaction rate amplification ratio is described below:

Procedure

1. Select values for $\bar{t}$, $\bar{r}_F$, $\bar{r}_O$, $\overline{r_F'^2}$, $\overline{r_O'^2}$, $\overline{t'^2}$
2. Calculate the three covariances using equation (39) and a value of the correlation coefficient of -0.9.
3. Use Newton's Method to solve for the constant coefficients of equation (40).
4. Choose values for B, T_A, T_{MIN}, T_{MAX}.
5. Numerically integrate equation (52) to calculate Z .

The values chosen for A, B, T_A, T_{MIN}, T_{MAX}, C_F°, C_O° are given in Table 1. Selected results of the parameter study undertaken are presented in the next section.

4. Results

4.1 Selected Results of the Most-Likely Bivariate Pdf For Two Species

All numerical integrations are performed with the use of Simpson's Rule. The number of subintervals on the integration interval of [0,1] are large enough so that no truncation error is incurred. The resulting value of Z_r' is accurate to five places.

In addition to the limitations of the program from Newton's Method, convergence problems were found from three other causes:

1. The value of $(\lambda_2 + \lambda_3 t)$ was a term close to zero in the denominator.
2. The value of the pdf became greater than 1×10^{38}, or less than 1×10^{-38}. This can be caused from a poor initial guess, or extreme values of the parameters.
3. The last problem was from one of the constraint equations. Equation (32) can re rewritten as:

$$\int_0^1 \int_0^1 r_F r_O \, p(r_F, r_O) \, dr_F dr_O = \overline{r_F' r_O'} + \bar{r}_F \bar{r}_O \qquad (53)$$

Since $\overline{r_F' r_O'}$ is always a negative term, for certain values of the parameters the right hand side is less than zero. This violates statistical theory and hence no convergence is possible for these values.

Figures 1 - 4 show the variation of Z_r' with increasing mean square fluctuations at constant mean species concentrations. As the fluctuations increase, Zr' always decreases. The lower limit of Z r' is zero, the case where there is no reaction. This will occur when the turbulence is so great that the fluctuations

inhibit the reaction, or where one of the species is not present.

Because of the convergence problems indicated with the computer program, results for high values of the mean square fluctuations were linearly extrapolated. Once a value of zero was reached, it remained zero for all higher values of mean square fluctuations. For the upper values of mean species concentrations Zr' is approximately constant and approaches a value of 1.0.

Figure 5 shows the variation of Zr' vs mean species concentration for constant values of mean square fluctuations. The value of Zr' increases with increasing mean species concentration.

4.2 Preliminary Results for the Full Three-Variable Model

To decrease the computer time to calculate each Z value for the full three-variable model, an exact transformation was used. The triple integrals, which must be calculated to use Newton's Method for non-linear systems, where reduced to double integrals where the variables are separable. All of the double integrals have the following form:

$$\int_T f(T) \int_{\sigma=f(T)} \sigma^N e^{-(L/4)\sigma^2} d\sigma \; dT \qquad (54)$$

where N = 0, 1, 2, 3, 4

The augmented matrix for Newton's Method and a sample derivation of a double

integral will be in a future progress report. When N = 0, the integral over σ is a scaled Version of the bell shaped curve. For N = 1, 2, 3, or 4, the integral over σ is a function of σ and the bell shaped curve.

One of the mathematical difficulties of Newton's Method is that convergence of this method is dependent on an initial guess within acceptable bounds of the exact answer.

As a first step toward an initial guess subroutine, restrictions were placed on the variables to reduce the full three-variable model to the two-variable model. (Note: In the following discussion, t is dimensionless temperature and r and x are dimensionless mean species concentrations A and B).

The restrictions on the three-variable model are $\bar{t} = \bar{r}$ and $\bar{t}'^2 = \bar{r}'^2$. t and r can be considered dummy variables since they are integrated over the same limits. Therefore let t = r = y. The pdf can now be written as:

$$\text{pdf} = \exp(\tfrac{1}{2}\lambda_0 + \lambda_1 y + \lambda_4 y^2) \cdot \exp(\tfrac{1}{2}\lambda_0 + \lambda_2 y + \lambda_3 x + [\lambda_5 + \lambda_6] yx) \tag{55}$$

This now gives a value for the pdf which can be evaluated from the one and two-variable pdf's. The initial guess subroutine can be developed by using power series around exact solutions.

In the model where $Z = Z_t Z_r$, t is not a function of either r or x (species A or B). Therefore, the integral over t can be placed inside the double integral

over r and x and Z can be calculated from:

$$Z = {}_0\int^1 {}_0\int^1 {}_0\int^1 Q \quad \exp(\lambda''_0 + \lambda''_1 t + \lambda''_2 t^2)$$
$$\cdot \exp(\lambda'_0 + \lambda'_1 t + \lambda'_2 x + \lambda'_3 rx) \quad dxdrdt \qquad (56)$$

where $Q = rx \exp\left[\frac{-10116}{K_1 t + K_2}\right] (k_1 t + k_2)^B$

Z for the full three variable model under the restrictions indicated for equation (55) can be calculated from:

$$Z = {}_0\int^1 {}_0\int^1 \exp\left[\tfrac{1}{2}\lambda_0 + \lambda_1 y + \lambda_4 y^2\right]$$
$$\cdot \exp\left[\tfrac{1}{2}\lambda_0 + \lambda_2 y + \lambda_3 x + (\lambda_5 + \lambda_6) yx\right] dydx \qquad (57)$$

Comparison of the Z value for the three variable model and Z calculated by multiplying the one-variable temperature only pdf by the two-variable bivariate pdf for two species can be evaluated by taking the difference between the values and determine if it can be made arbitrarily small. In equation form:

$$Z - Z_t Z_r = {}_0\int^1 {}_0\int^1 {}_0\int^1 \{e^{\lambda_0 + \lambda_1 t + \lambda_2 r + \lambda_3 x + \lambda_4 tr + \lambda_5 tx + \lambda_6 rx}$$
$$- \exp(\lambda''_0 + \lambda''_1 t + \lambda''_2 t^2) \exp(\lambda'_0 + \lambda'_1 r + \lambda'_2 x + \lambda'_3 rx)\} dxdrdt \qquad (58)$$

Under the restrictions of $\bar{t} = \bar{r}$ and $\bar{t}'^2 = \bar{r}'^2$, the difference between the Z values is exactly zero, if the correlation coefficients are as follows:

$$\rho_{tr} = +1.0$$
$$\rho_{tx} = -0.9$$
$$\rho_{rx} = -0.9$$

There are no restrictions placed on species concentration B ($\bar{x}, \bar{x}'^2$).

5. Conclusions and Direction for Future Work

5.1 Conclusions

5.1.1 Effects of Species Fluctuations on the Reaction Rate

The effects of species concentration fluctuations on the reaction rate are assessed by treating the species concentrations as continuous random variables. A joint pdf is used to relate the variables. The total amplification ratio is the mean turbulent reaction rate divided by the corresponding laminar value. The reaction rate amplification ratio, which only accounts for the effects of species concentrations, is discussed here. The results obtained for a parameter study on Zr' are the following:

1. The value of Zr' is between 0 and 1.0.

2. For constant values of mean species concentrations of A and B ($\bar{r}_A$, $\bar{r}_B$) and for constant fluctuations of species A ($\bar{r}_A'^2$), Zr' always decreases as fluctuations of species B($\bar{r}_B'^2$) increases.

3. For constant values of fluctuations for species A and B and for constant mean species concentration of A, Zr increases as $\bar{r}_A$ increases.

5.2 Direction for Future Work

1. Having exact answers to the three variable model, evaluate the error in the program and write an initial guess subroutine.

2. See how Z compares to Zt + Zr for all of the mean quantities not equal.

3. Compare Z vs $Z_t \cdot Z_r$ for different correlation coefficients. One suggestion is to set the value of the correlation coefficient between species equal to -0.9 and between temperature and species equal to -0.99. These values were suggested by Antaki [1].

AN INVESTIGATION OF THE RANGES OF APPLICABILITY OF CHEMICAL KINETIC MODELS OF HYDROGEN-AIR COMBUSTION

Introduction

The study of hydrogen fueled supersonic combustion ramjets (scramjets) has been a major project in the research programs of the Langley Research Center. A large computer program was developed which solves flowing or static chemical kinetic problems involving many chemical species (Ref. 7). The program uses the conservation equations (Ref. 8) for one-dimensional steady-state flow to analyze a complex reacting gas mixture flowing through an arbitrarily assigned area.

It is known that the computational time requirement for this computer program is proportional to the number of species and reactions being treated. It is the purpose of this task to develop a method which reduces these numbers in the study of hydrogen-air combustion and at the same time preserve the correct physical-chemical behavior. The result of this work will be to reduce computer time requirements.

The method that will be used in this paper will be an extension and refining of the method proposed by Shinitt (Ref.9). This method involves the tracking of a "trigger" species which is used to determine whether the flow is in an "ignition" mode or in a "combustion" mode. Ignition and combustion are defined in the classical sense. Ignition delay time is taken to be the time required for the temperature increase to reach five percent of the overall temperature increase.

$$T_{ignition} = T_{initial} + 0.05(T_{equilibrium} - T_{initial})$$

When the temperature is less than $T_{ignition}$, the flow is in the "ignition" mode. Otherwise, the flow is in the "combustion" mode (see figure 6).

This work will try to show that while an extensive chemical package is needed to describe the "ignition" mode, a smaller package is sufficient to deal with the "combustion" mode. Evans and Schexnayder concluded that a 25 reaction system involving 12 species (referred to as 25(12)) was required to describe "ignition" processes while an 8(7) system sufficed to deal with the "combustion" mode (Ref.10). This paper will try to minimize the computational time requirements once the "combustion" process is initiated (i.e. a smaller package or one that takes less computational time than the 8(7) system might suffice to deal with the "combustion" mode).

A 37(13) system will be used as the "test" chemical kinetic package (Table 2). Any system with smaller numbers will be "tested" against the 37(13) system to see if the correct physical-chemical behavior is preserved. This will be accomplished in the following way. First, the full 37(13) system will be run from the initial state to equilibrium. Next the test system will be run from the point where the "combustion" in the 37(13) system initiates. The test system's initial values (pressure, temperature, equivalence ratio, chemical composition) will be that of the 37(13) system's values at the point of combustion. Temperature-time profiles and chemical behaviors will be compared (see figure 7). If the difference between the 37(13) system and the test system is within an acceptable range then the test system will be

sufficient to deal with the "combustion" process.

An 8(7) system (Table 3) will be tested to confirm the results of Evans and Schexnayder. In order to further reduce computational time, a 2(4) global model (Table 4) developed by Chinitz and Rogers (Ref.11) will be tested. Lastly the paper will try to test the partial equilibrium assumption (Ref.12) on the above systems in an effort to absolutely minimize computational time. To accomplish this, a large number of one-dimensional constant pressure, H_2 - air computations will be performed in the range:

$$0.5 \leq \phi \leq 1.5$$

$$850 \leq T \leq 1200$$

$$0.5 \leq p \leq 1.0$$

where ϕ is the equivalence ratio, T the temperature in ^{o}R, and p the pressure in atmospheres. A list of these individual cases is given in Table 5.

Plots of the mole fraction of the trigger species versus ignition time and ignition time versus ignition temperature will be made in accordance with the process described in reference 9.

Preliminary Results

The major problem in the first semester of work had been in the operation of the computer program. The program had been running smoothly on the N. Y. U. operating system until the system was switched to a CYBER. At present the program is not working but will be operating within the next few weeks. As a result progress has been slow.

The first 35 of the 45 cases have been run using the extensive 37(13) package. Cases 16-21 using this package were terminated due to excessive computer running times. This problem has been encountered before in other studies.

Fifteen cases have been run using the 8(7) from ignition to equilibrium. Figures 8-12 show the 8(7) system compared to the 37(13) system at a pressure of one atmosphere, an equivalence ratio of 0.5, and various temperatures. This set of comparisons is typical of the results found in comparing the 8(7) system with the 37(13) system for the entire process. At 850°K and 900°K the 8(7) system lags behind the 37(13) system. For temperatures of 1000°K, 1100°K, and 1200°K the 37(13) system lags behind the 8(7) system. Therefore, between 900°K and 1000°K a transition takes place. As a result there is a temperature range at approximately 950°K where the 8(7) system describes both the ignition and combustion processes.

Figure 13 shows the comparison of the 37(13) and the 8(7) systems in the combustion mode. As shown by Evans and Schoonmaker the 8(7) system describes the combustion process. More runs of the 8(7) system starting at the combustion point

of the 37(13) system are needed for further verification.

Figure 14 shows a logarithmic plot of mole fraction of OH versus ignition time. As shown in reference 9 the plot is linear and is thereby a good trigger species. More test cases will be needed to verify this.

Figure 15 shows a semilogarithmic plot of ignition time versus the reciprocal of initial temperature for both the 8(7) and 37(13) systems. The results here confirm the work of Rogers and Schexnayder.

Conclusions and Observations

These are preliminary conclusions based only on the initial work done so far:

1. The 8(7) system does not describe the entire process (i.e. ignition and combustion) except at 950°K, one atmosphere, and an equivalence ratio of 0.5.
2. The 8(7) system describes the combustion process.
3. At one atmosphere and an equivalence ratio of 0.5 the logarithmic plot of mole fraction of OH versus ignition time is linear.
4. At the same conditions as above, the effect of initial temperature on ignition time for the 37(13) package confirms the results of reference 8.

FLAME STABILIZATION STUDIES USING A PERFECTLY-STIRRED REACTOR MODEL

The use of the stirred reactor concept to model combustion regions of intense mixing and recirculation dates to Longwell, et. al. (Refs. 12 and 13). Longwell's laboratory stirred reactor, along with regions in a SCRAMJET engine which may be modeled using stirred reactor theory, is shown in Fig. 16. Reactors in which reactants and inerts exist in the gas phase only are termed "perfectly stirred"; multi-phase systems are "well-stirred."

A version of the perfectly-stirred reactor code developed by Pratt (Ref. 14) was used along with chemical kinetic mechanisms developed at LRC for hydrogen, hydrocarbon and silane combustion (e.g. Refs 8, 15, and 16) to investigate blowout limits for neat fuels and for mixtures of these fuels. Results are shown in Figs. 17 through 27. The blowout limit, in all cases, was determined by examining computed curves of reactor temperature as a function of the mass flow rate per unit reactor volume, $\dot{m}/V$. The blowout limit was then determined as suggested in the sketch below:

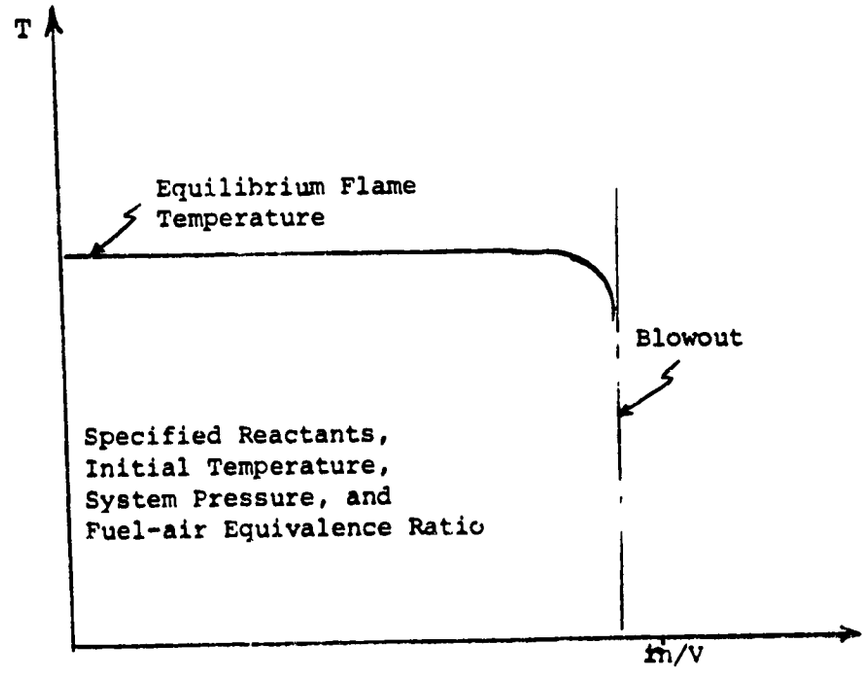

The residence time in the reactor, related to $\dot{m}/V$ by

$$t_R = \rho/(\dot{m}/V)$$

is simultaneously calculated in the computer code. (Note that a recent criterion for blowout developed by R. C. Rogers was not available at the time the calculations reported upon herein were made.)

Fig. 17 illustrates the effect of initial reactant temperature and quantity of silane in the fuel on minimum residence times required to avoid blowout of the flame. These results are for H_2 and CH_4 as the principal fuel constituents. It is of interest that increasing SiH_4 in the fuel results in a more substantial effect for H_2 than for CH_4. On the other hand, the results for H_2 suggest that, at high initial temperatures, little stabilizing effect is achieved for H_2/SiH_4 until the silane concentration exceeds 5% by volume. Increasing the initial temperature, as expected, increases the stable flame region. These same results may be noted by reference to the cross-plot in Fig. 18.

Figs. 19 and 20 illustrate the flame stabilizing effect of increasing the system pressure. As can be seen, the effect is substantial going from 0.2 atm to 2.0 atm wherein, at 1000°K for example, minimum required residence time decreases from about 7 μsec (at 0.2 atm) to about 1 μsec (at 2.0 atm).

The effect of equivalence ratio is indicated in Figs. 21 and 22 for a 20% SiH_4/80% H_2 fuel (by volume) at 1.0 atm. The stabilizing effect of increasing the equivalence ratio ϕ is seen to be predominant at the lower values of initial reactant temperature T_o. For example, at T_o = 600°K, t_R decreases from about 3×10^{-4} sec (ϕ = 0.2)

to about 3×10^{-6} sec ($\phi = 2.0$); a decrease of two orders-of-magnitude. On the other hand, at $T_o = 1200°K$, the decrease in t_R is from about 2 μsec ($\phi = 0.2$) to 0.5 μsec ($\phi = 2.0$).

The traditional stirred reactor plot of ϕ versus in/V is shown for SiH_4/H_2 fuels ($T_o = 600°K$, p = 1 atm) in Fig. 23. The stabilizing effect of increased silane concentrations is again noted. Of particular interest are the following:

1. The locus of maximum $\dot{m}/V$ values increases from $\phi = 1$ for pure H_2 to about $\phi = 2.5$ for pure SiH_4; and

2. A reversal occurs below $\phi = 1.0$ wherein the stable flame region is greater in extent for <u>lesser</u> quantities of silane in the fuel.

A possible explanation for these two findings is suggested in Table 6 where it is noted that the principal initiating reactions for silane oxidation are SiH_4 pyrolysis followed by the very rapid oxidation of the pyrolysis produce SiH_2. As seen, these two steps are <u>exothermic.</u> However, the direct step O_2 oxidation of SiH_4 to SiH_3 and HO_2 is mildly endothermic when compared with the highly endothermic steps which initiate the CH_4 and H_2 oxidation chains. Hence, high silane concentrations relative to oxygen (i.e., high ϕ values) tend to result in greater flame stability due to the exothermicity and relative rapidity of the principal chain-initiating steps.

On the other hand, below $\phi = 1$ flame stability is favored by the higher exothermicity of the overall reaction (Table 6, $\phi<1$). Since the heat of combustion of silane is substantially below that of hydrogen and even the hydrocarbons, at low equivalence ratios increased silane concentrations appear to have a destabilizing effect.

A similar result is seen in Fig. 24 where SiH_4/CH_4 blowout limits are shown. Fig. 25 again suggests the picture detailed above. For example, the activation energy of the reaction

$$CH_4 + M \rightarrow CH_3 + H + M$$

is given in Ref.16 as about 85,755 Kcal/gmole, while for

$$C_3H_8 + M \rightarrow CH_3 + C_2H_5 + M$$

it is given as 64,968 Kcal/gmole. Hence, the relative rapidity of the latter tends to favor C_3H_8 at $\phi>1$. On the other hand, the higher heat of combustion of methane favors it at $\phi<1$. These predicted trends are verified in Fig. 25.

Figs. 26 and 27 summarize the results obtained for the neat fuels in terms of residence time (Fig. 26) and $\dot{m}/V$ (Fig. 27). In general, for $\phi>1$ flame stabilization is favored by the use of silane in the fuel mixture and by the use of the higher hydrocarbons (above CH_4). For $\phi<1$, silane may serve to reduce flame stability and the use of methane is favored over the higher hydrocarbons. Also favoring flame stability are high initial reactant temperatures and high pressures.

REFERENCES

1. Antaki, P. J., "The Effects of Temperature and Species Fluctuations on Reaction Rates in Turbulent Reacting Flows." M. E. Thesis, The Cooper Union, School of Engineering, April 1981.

2. Foy, E., "The Effects of Temperature and Species Fluctuation on Reaction Rates in Turbulent Reacting Flows." M.E. Thesis, The Cooper Union, School of Engineering, April 1982.

3. Meyer, P.D., Introductory Probability and Statistical Applications, Second Edition, Addison-Wesley Publishing Co., Reading, MA, 1972.

4. Pope, S. B., "A Rational Method of Determining Probability Distributions on Reaction Rates in Turbulent Reacting Flows," J. Non-Equilib. Thermo., V.4, 1979, pp. 309-320.

5. Ronan, G., "Selection Process Between Probability Density Functions that Model the Temperature Fluctuations in Turbulent Reacting Flows," M. E. Thesis, The Cooper Union, School of Engineering, April 1982.

6. Goldstein, D., "Effects of Temperature and Species Fluctuations on Reaction Rates in Turbulent Reacting Flows," Special Report, The Cooper Union, School of Engineering, April 1982.

7. McLain, Allen G. and Rao, C.S.R., "A Hybrid Computer Program for Rapidly Solving Flowing or Static Chemical Kinetic Problems Involving Many Chemical Species", NASA TM X-3403, July 1976.

8. Rogers, R. C. and Schexnayder, C.M. Jr., "Chemical Kinetic Analysis of Hydrogen-Air Ignition and Reaction Times", NASA Technical Paper 1856, July 1981.

9. Chinitz, W., "Simplifying Chemical Kinetic Analyses of Reacting Flows Using an Ignition-Combustion Model".

10. Evans, J. S. and Schexnayder, C.J. Jr., "Critical Influence of Finite Rate Chemistry and Unmixedness on Ignition and Combustion of Supersonic H_2-Air Streams", AIAA Paper #79-0355, Jan. 1979.

11. Rogers, R. C. and Chinitz, W., "On the Use of a Global Hydrogen-Air Combustion Model in the Calculation of Turbulent Reacting Flows", AIAA Paper #82-0112, Jan. 1982.

12. Longwell, J. P.; Frost, E. E. and Weiss, M.A., "Flame Stability in Bluff Body Recirculation Zones", I. and E. Chem., 45, 8, Aug. 1953.

13. Longwell, J. P. and Weiss, M.A., "High Temperature Reaction Rates in Hydrocarbon Combustion," I. and E. Chem, 47, 8, Aug. 1955.

14. Pratt, D. T., "PSR - A Computer Program for Calculation of Steady Flow, Homogeneous Combustion Reaction Kinetics", Bulletin 336, Wash. State Univ., 1974.

15. McLain, A. G. and Jachimowski, C. J., "Chemical Kinetic Modeling of Propane Oxidation Behind Shock Waves", NASA TN D-8501, July 1977.

16. Jachimowski, C. J. and Wilson, C. H., "Chemical Kinetic Models for Combustion of Hydrocarbons and Formation of Nitric Oxide," NASA TP 1794, Dec. 1980.

Nomenclature

A	pre-exponential constant
B	temperature exponent
C	instantaneous concentration
C°	initial concentration
E(x)	expected (mean) value of x
F	denotes a fuel species
f(x, y)	joint probability density function of (x, y).
g(x, y)	function of the two-dimensional continuous random variable (x, y)
$\overline{g(x, y)}$	mean value of g(x, y)
h(x)	function of the continuous random variable, x
k	Arrhenius reaction rate constant
k_1, k_2	constants dependent upon T_{min} and T_{max}
k_l	laminar Arrhenius reaction rate constant
$\overline{k_t}$	mean turbulent Arrhenius reaction rate constant
m	constant, defined in equation (30)
max	denotes maximum value
min	denotes minimum value
n	order of reaction constant
O	denotes oxidizer species
P	denotes a product species
p(x)	probability density function of x
p(x, y)	joint probability density function of (x, y)
r	dimensionless concentration and constant defined by equation (30)

$\bar{r}$	mean dimensionless concentration
$\overline{r'^2}$	mean square fluctuation of dimensionless concentration
t	dimensionless temperature
$\bar{t}$	mean dimensionless temperature
$\overline{t'^2}$	mean square fluctuation of dimensionless temperature
T	temperature
T_A	activation temperature
$V(x)$	variance of x
$\dot{w}$	reaction rate
$\dot{w}_l$	laminar reaction rate
$\bar{\dot{w}}_t$	mean turbulent reaction rate
Z	reaction rate constant amplification ratio
Z'	reaction rate amplification ratio
Γ	gamma function
μ_x	mean of a continuous random variable, x
μ_k	kth moment of a random variable
σ^2	variance of a continuous random variable
ρ	correlation coefficient

Table 1. Case Data

Case No.	B	T_A (°K)	T_{max} (°K)
1	0	10116	2500
2	0	5000	2500
3	1	10116	2500
4	0	10116	3000

Note: $A = 8.4 \times 10^{13}$, $T_{min} = 500°K$, for all cases.

Table 2 - 37(13) SYSTEM

REACTION NUMBER	REACTION						
1	[illegible]	+	1*C2	=	1*C	+	1*C
2	[illegible]	+	1*H2	=	1*H	+	1*H
3	[illegible]	+	1*H2O	=	1*H	+	1*OH
4	1*H	+	1*O2	=	1*HO2	+	[illegible]
5	[illegible]	+	1*NO2	=	1*NO	+	1*O
6	[illegible]	+	1*NO	=	1*N	+	1*O
7	[illegible]	+	1*H2O2	=	1*OH	+	1*OH
8	[illegible]	+	1*O3	=	1*O2	+	1*O
9	1*O	+	1*H	=	1*OH	+	[illegible]
10	1*H2O	+	1*O	=	1*OH	+	1*OH
11	1*H2	+	1*OH	=	1*H2O	+	1*H
12	1*O2	+	1*H	=	1*OH	+	1*O
13	1*H2	+	1*O	=	1*OH	+	1*H
14	1*H2	+	1*O2	=	1*OH	+	1*OH
15	1*H	+	1*HO2	=	1*H2	+	1*O2
16	1*H2	+	1*O2	=	1*H2O	+	1*O
17	1*H	+	1*HO2	=	1*OH	+	1*OH
18	1*H2O	+	1*O	=	1*H	+	1*HO2
19	1*O	+	1*HO2	=	1*OH	+	1*O2
20	1*OH	+	1*HO2	=	1*O2	+	1*H2O
21	1*H2	+	1*HO2	=	1*H2O	+	1*OH
22	1*HO2	+	1*H2	=	1*H	+	1*H2O2
23	1*H2O2	+	1*H	=	1*OH	+	1*H2O
24	1*H2	+	1*OH	=	1*O	+	1*H2O
25	1*H2	+	1*H2O	=	1*OH	+	1*H2O2
26	1*HO2	+	1*HO2	=	1*H2O2	+	1*O2
27	1*O	+	1*O3	=	1*O2	+	1*O2
28	1*O3	+	1*NO	=	1*NO2	+	1*O2
29	1*O3	+	1*H	=	1*OH	+	1*O2
30	1*O3	+	1*OH	=	1*O2	+	1*HO2
31	1*O	+	1*NO2	=	1*NO	+	1*O2
32	1*H	+	1*NO2	=	1*OH	+	1*NO
33	1*O	+	1*NO2	=	1*O2	+	1*NO
34	1*HO2	+	1*H	=	1*OH	+	1*OH
35	1*NO2	+	1*O	=	1*NO	+	1*O2
36	1*HO2	+	1*NO	=	1*NO2	+	1*OH
37	1*O3	+	1*HO2	=	2*O2	+	1*OH

Table 3 - S(7) System

REACTION NUMBER	REACTION						
1		+	1*C2	=	1*C	+	1*C
2		+	1*H2	=	1*H	+	1*H
3		+	1*H2O	=	1*H	+	1*O
4	1*C	+	1*H	=	1*CH	+	
5	1*H2O	+	1*C	=	1*CH	+	1*O
6	1*H2	+	1*CO	=	1*H2O	+	1*
7	1*CO	+	1*H	=	1*CH	+	1*O
8	1*H2	+	1*O	=	1*OH	+	1*H

Table 4 - 2 Step Global Model

$$H2 + O2 \xrightarrow{k_{g1}} 2*OH \qquad (1)$$

$$2*OH + H2 \xrightarrow{k_{g2}} 2*H2O \qquad (2)$$

Table 5 - 45 CASES

CASE	V	I, AMP	T_e, ^oK
1	0.5	0.5	850
2	0.5	0.75	850
3	0.5	1.0	850
4	0.5	0.5	900
5	0.5	0.75	900
6	0.5	1.0	900
7	0.5	0.5	1000
8	0.5	0.75	1000
9	0.5	1.0	1000
10	0.5	0.5	1100
11	0.5	0.75	1100
12	0.5	1.0	1100
13	0.5	0.5	1200
14	0.5	0.75	1200
15	0.5	1.0	1200
16	1.0	0.5	850
17	1.0	0.75	850
18	1.0	1.0	850
19	1.0	0.5	900
20	1.0	0.75	900
21	1.0	1.0	900
22	1.0	0.5	1000
23	1.0	0.75	1000
24	1.0	1.0	1000
25	1.0	0.5	1100
26	1.0	0.75	1100
27	1.0	1.0	1100
28	1.0	0.5	1200
29	1.0	0.75	1200
30	1.0	1.0	1200

TABLE 6. HEATS OF REACTION OF ELEMENTARY AND OVERALL REACTIONS

REACTION	K_f @ 1500 K	ΔH_R°		
$SiH_4 \rightarrow SiH_2 + H_2$	[illegible] $\times 10^5$			$\phi > 1$
$SiH_2 + O_2 \rightarrow HSiO + OH$	2.91×10^{13}			
$SiH_4 + O_2 \rightarrow H_2 + HSiO + OH$		-1.2	kcal/mole	
$SiH_4 + O_2 \rightarrow SiH_3 + HO_2$	8.54×10^4	$+32.0$	"	
$CH_4 + M \rightarrow CH_3 + H + M$	3.79×10^4	$+101.9$	"	
$H_2 + M \rightarrow 2H + M$		$+104.2$	"	
$O_2 + M \rightarrow 2O + M$		$+119.2$	"	
$H_2 + O_2 \rightarrow 2OH$	5.96×10^6	$+19.0$	"	
$SiH_4 + 2O_2 \rightarrow SiO_2 + 2H_2O$		11,000	Btu/lbm fuel	$\phi < 1$
$CH_4 + 2O_2 \rightarrow CO_2 + 2H_2O$		25,600	"	
$H_2 + \frac{1}{2}O_2 \rightarrow H_2O$		51,011	"	

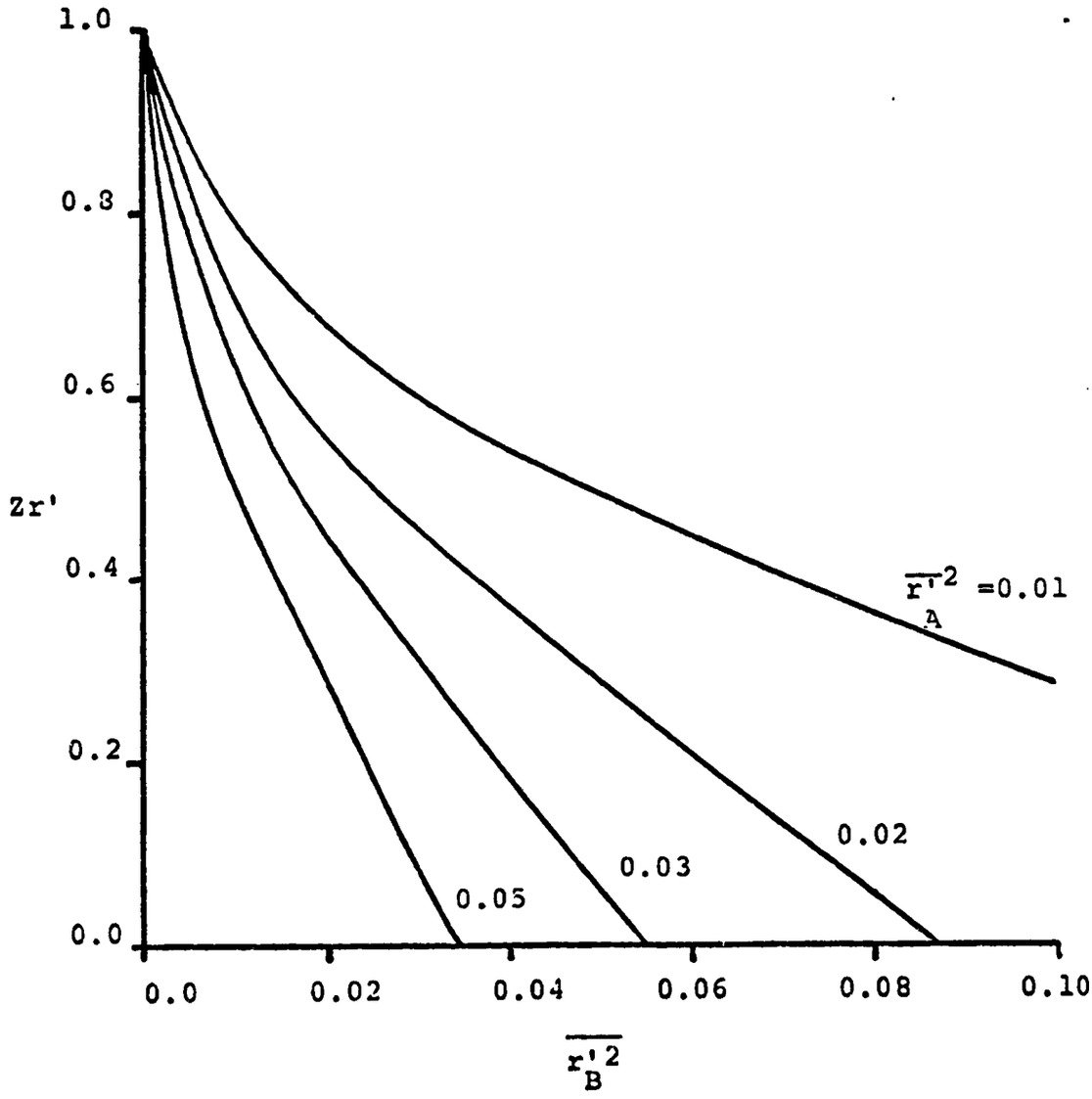

Figure 1: Variation of the reaction rate amplification ratio with mean square fluctuation for

$\overline{r_A} = 0.2$, $\overline{r_B} = 0.2$

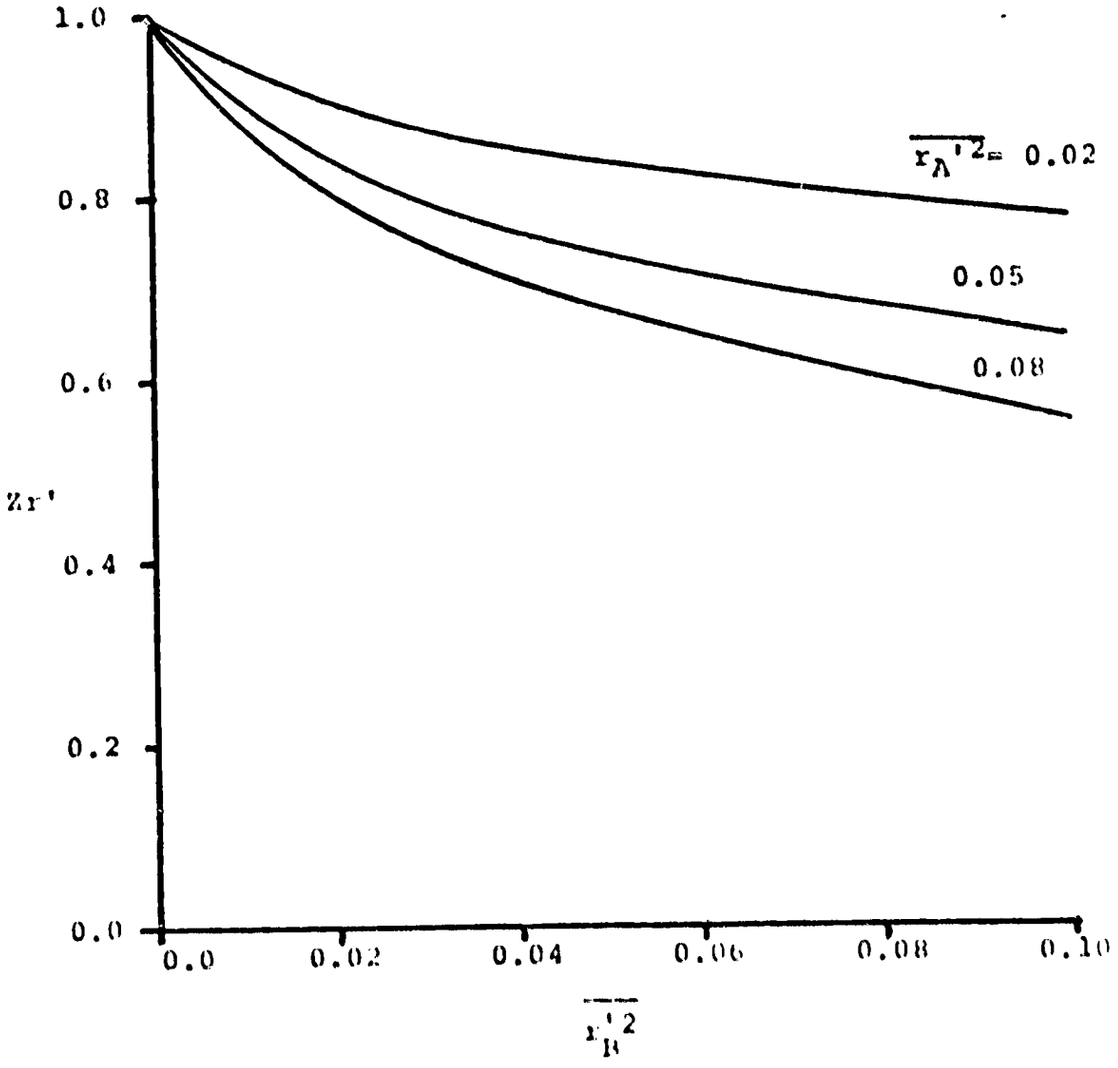

Figure 2: Variation of the reaction rate amplification ratio with mean square fluctuations for

$\overline{r_A}$=0.2 , $\overline{r_B}$ 0.9

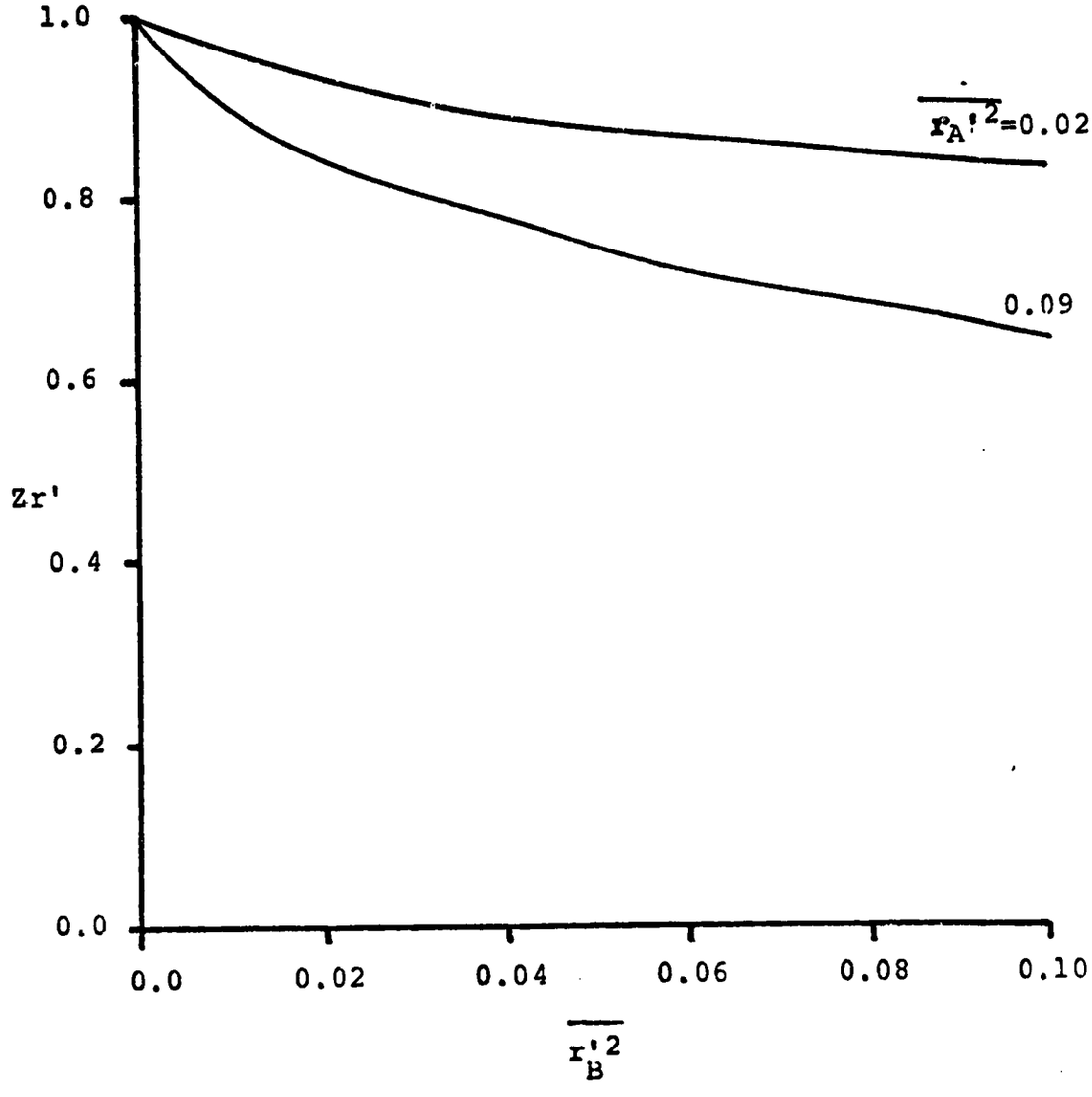

Figure 3: Variation of the reaction rate amplification ratio with mean square fluctuations for

$\overline{r_A}$=0.4 , $\overline{r_B}$= 0.6

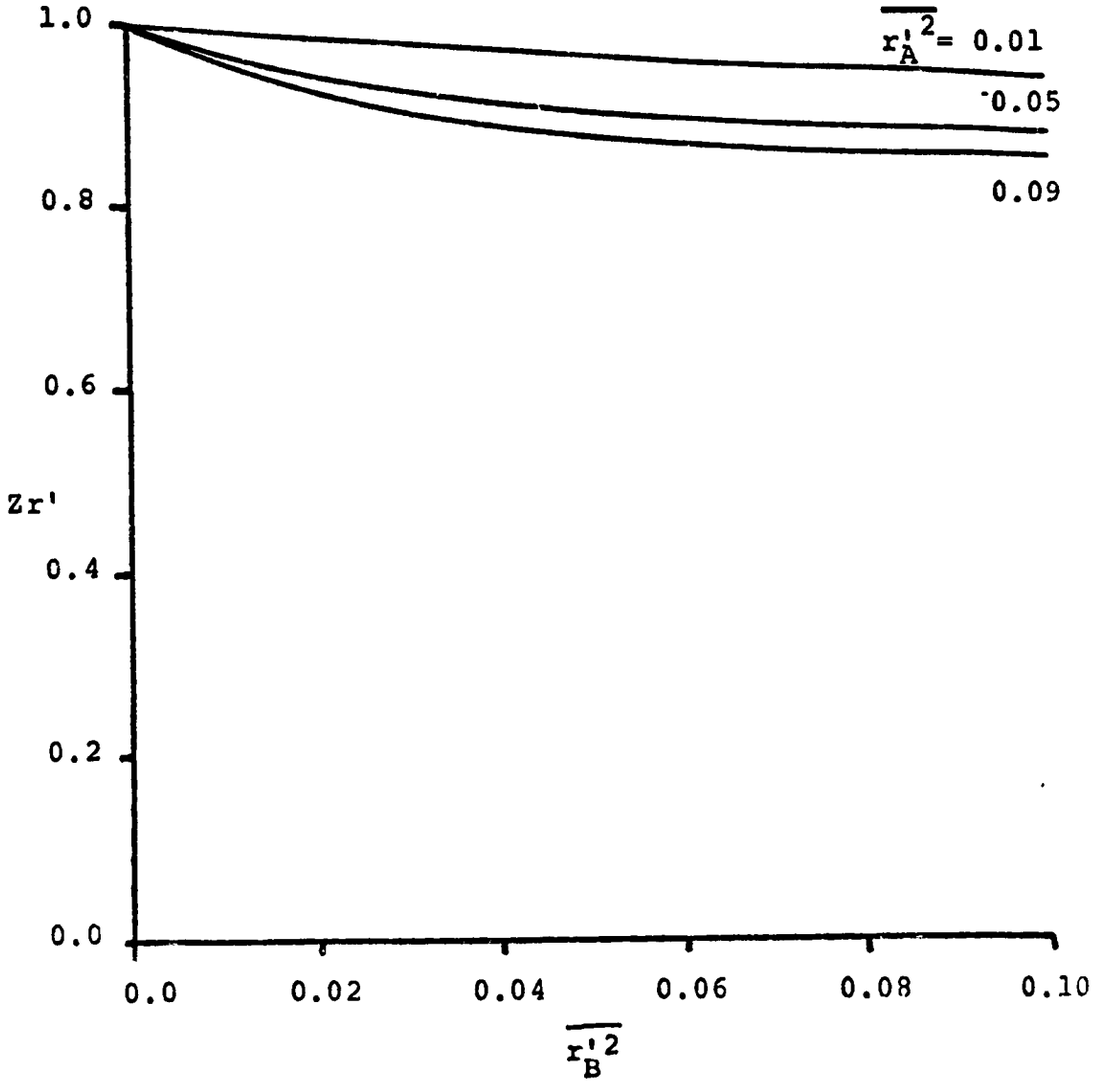

Figure 4: Variation of the reaction rate amplification ratio with mean square fluctuations for

$\overline{r_A}$=0.7 , $\overline{r_B}$=0.7

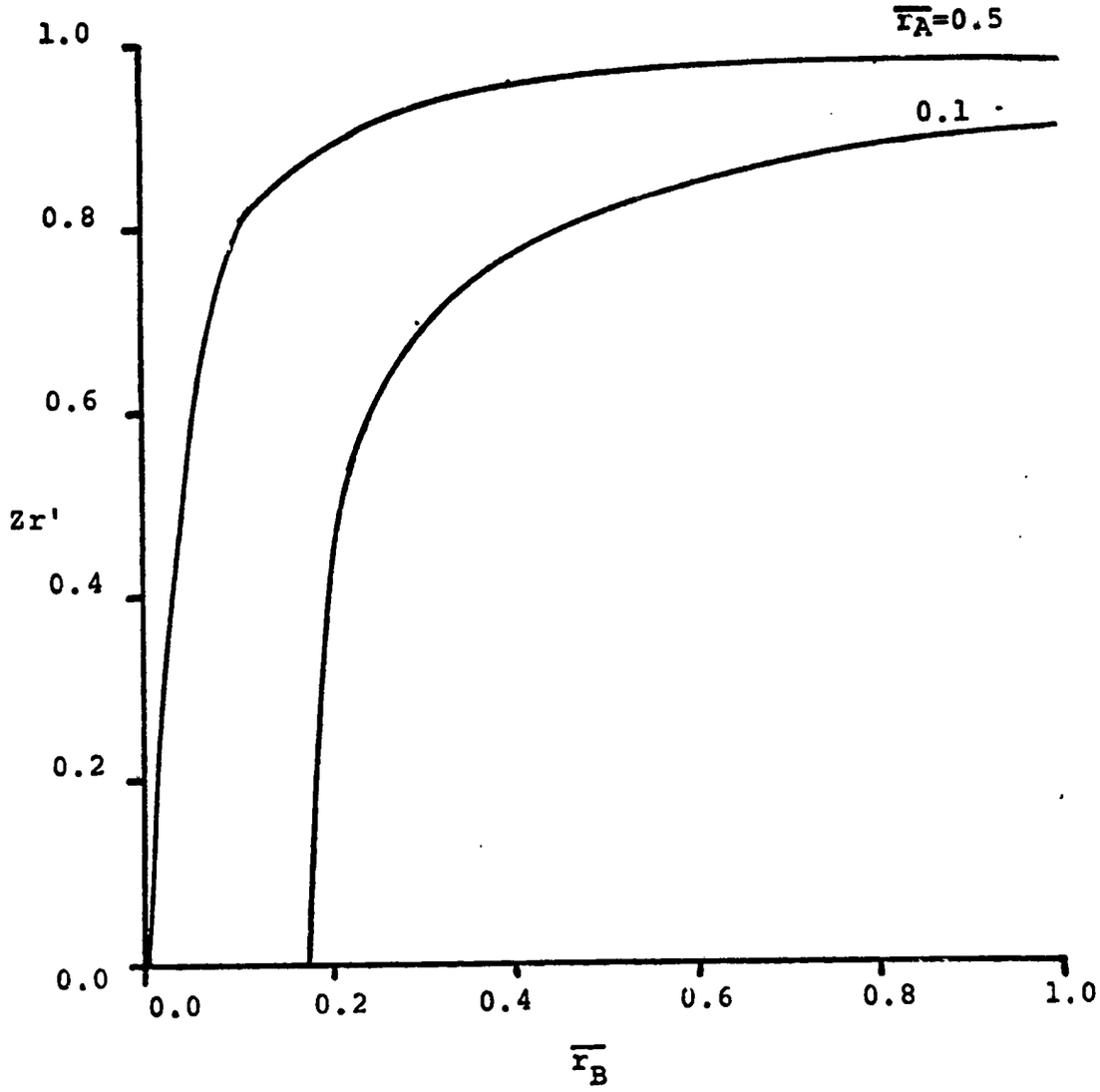

Figure 5: Variation of the reaction rate amplification ratio with mean species concentrations for $\overline{r_A'^2}=0.01$, $\overline{r_B'^2}=0.01$

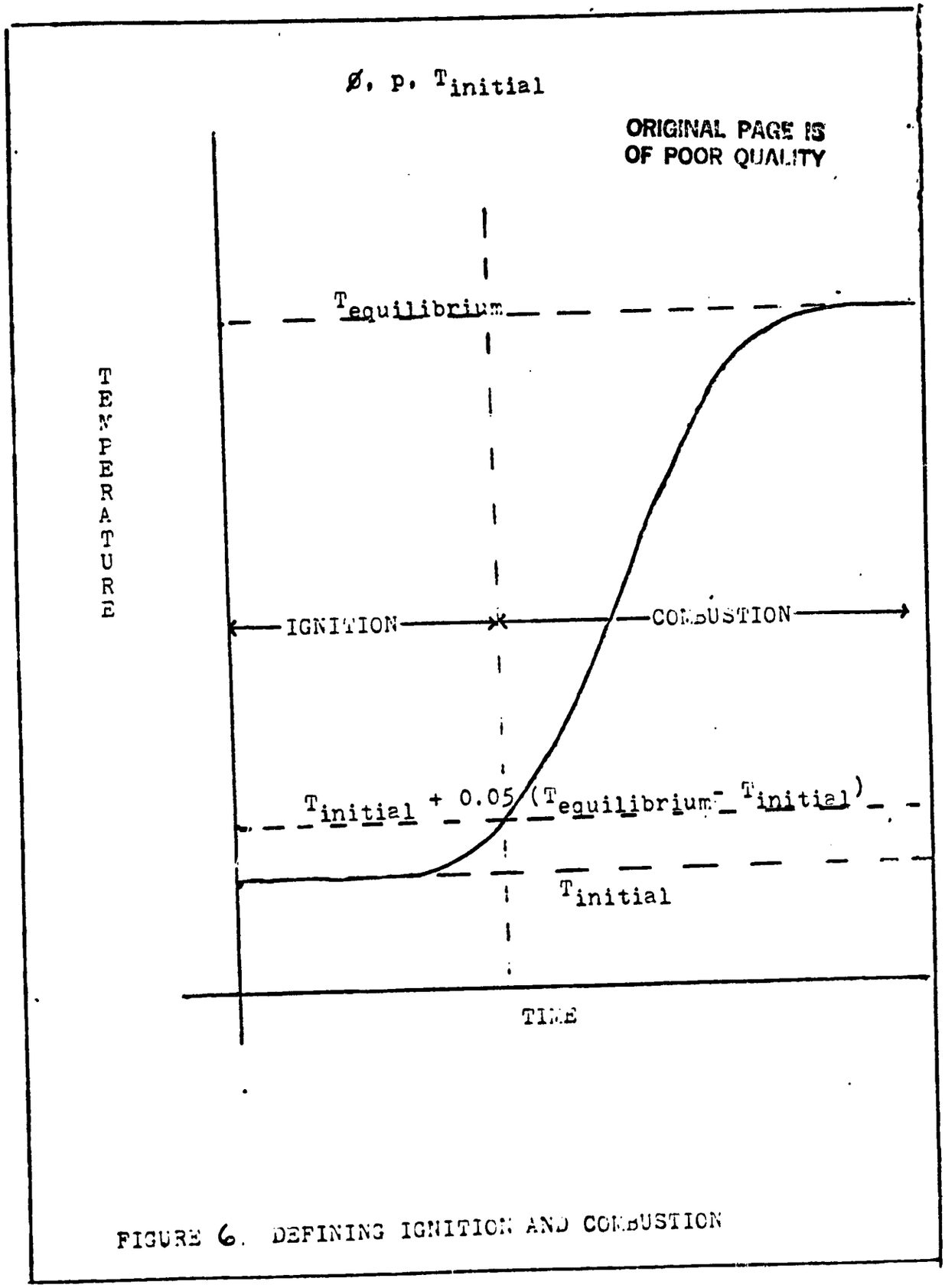

FIGURE 6. DEFINING IGNITION AND COMBUSTION

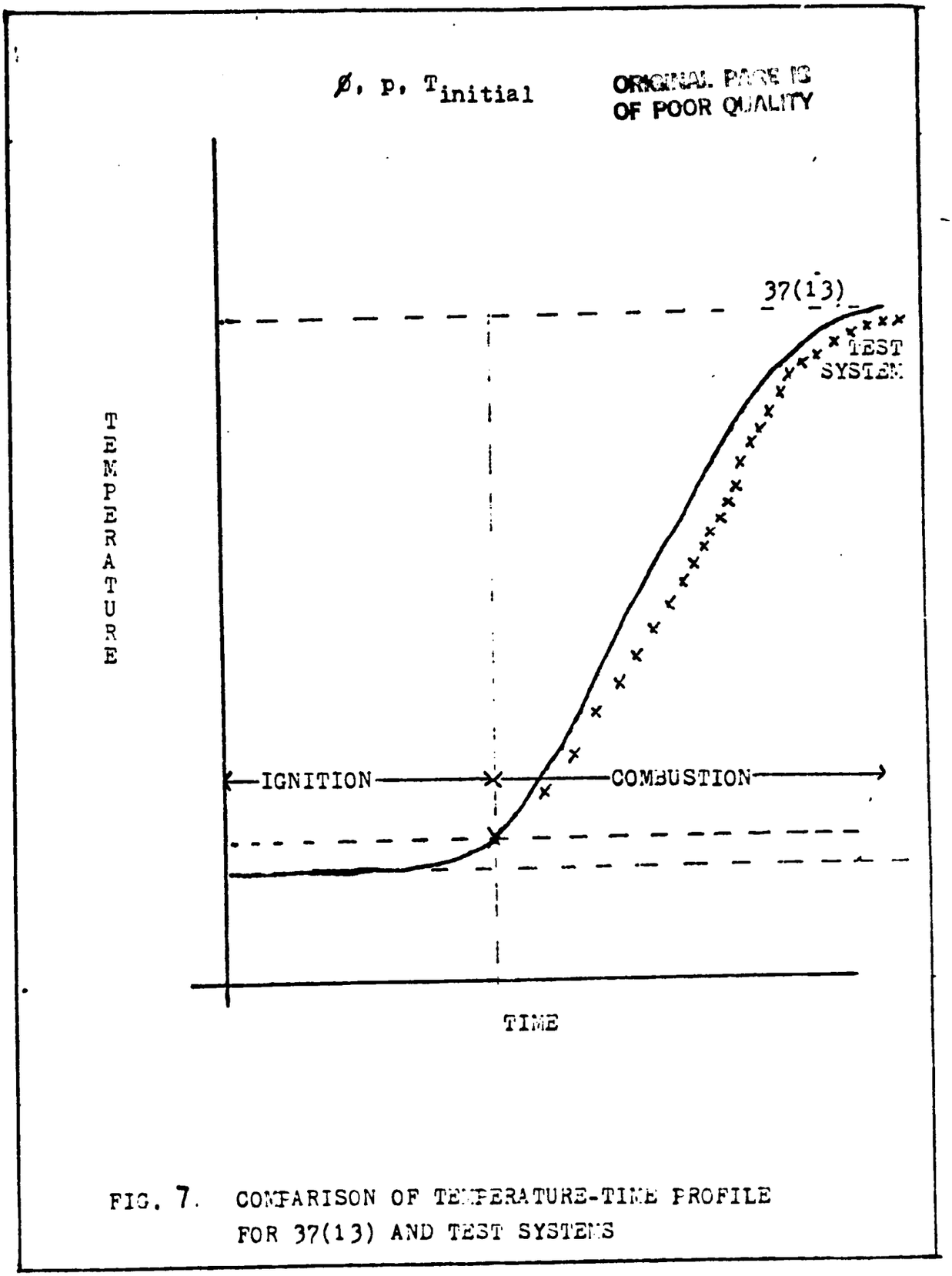

FIG. 7. COMPARISON OF TEMPERATURE-TIME PROFILE FOR 37(13) AND TEST SYSTEMS

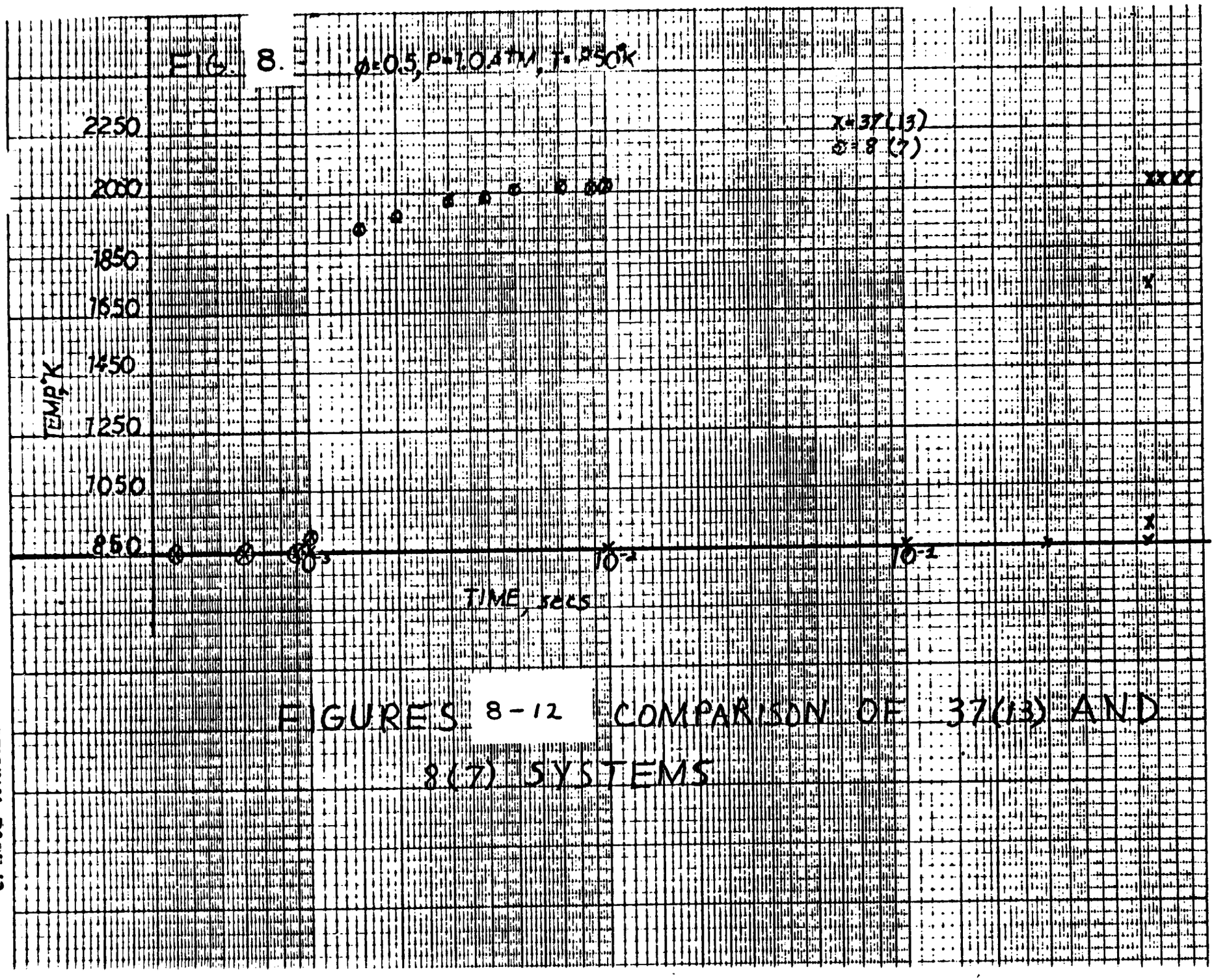

FIGURES 8-12 COMPARISON OF 37(13) AND 8(7) SYSTEMS

FIG. 9

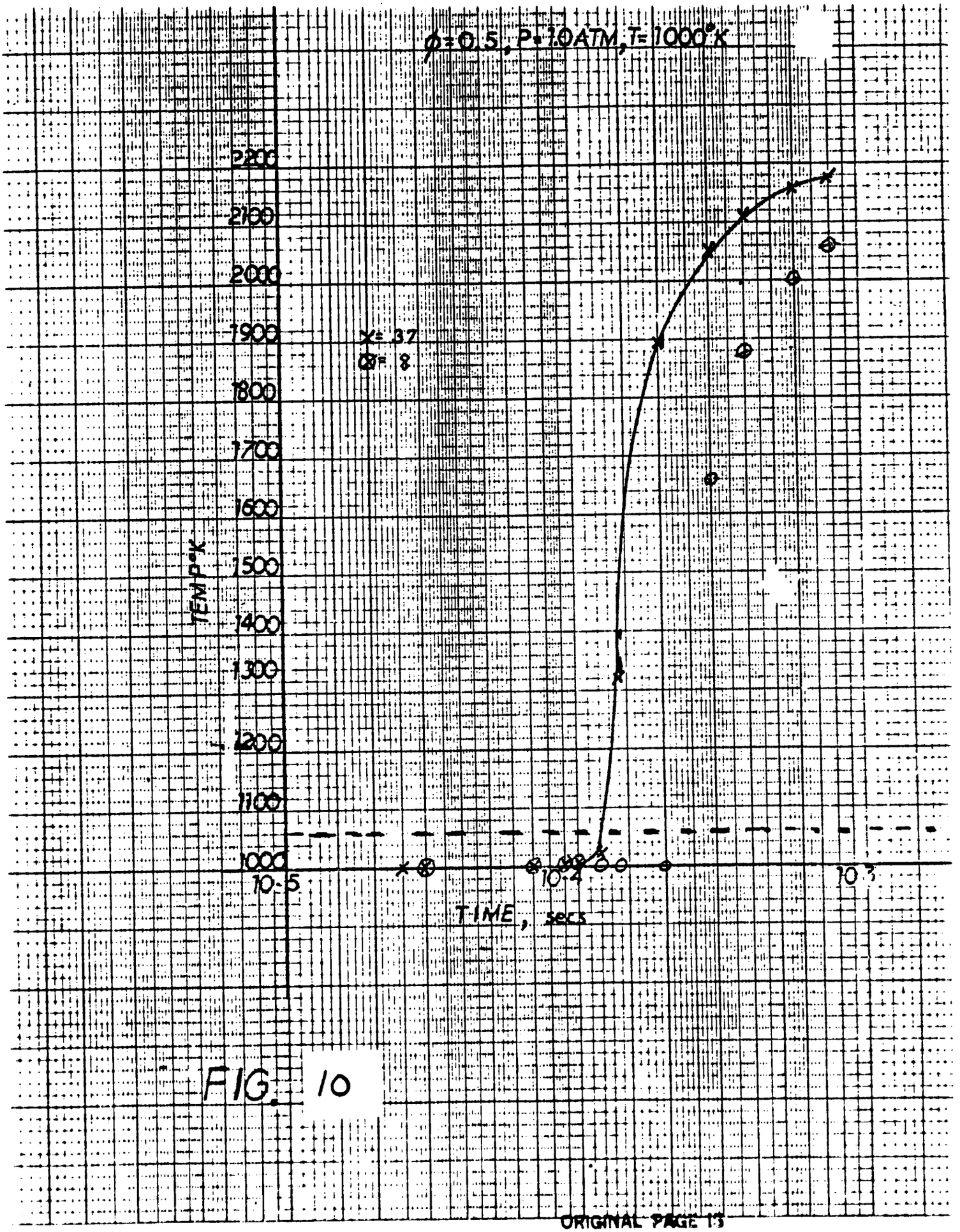

FIG. 10

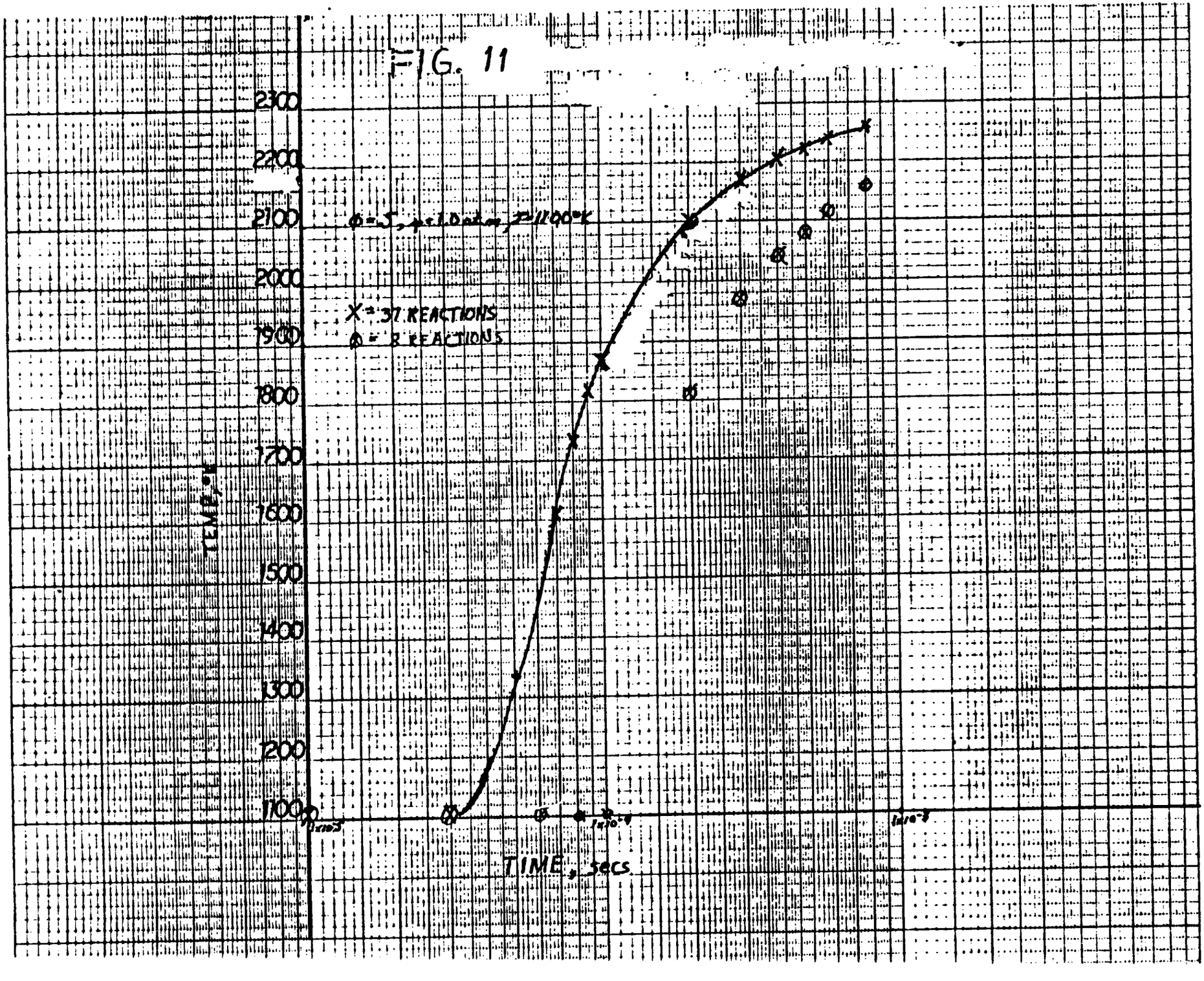

FIG 12

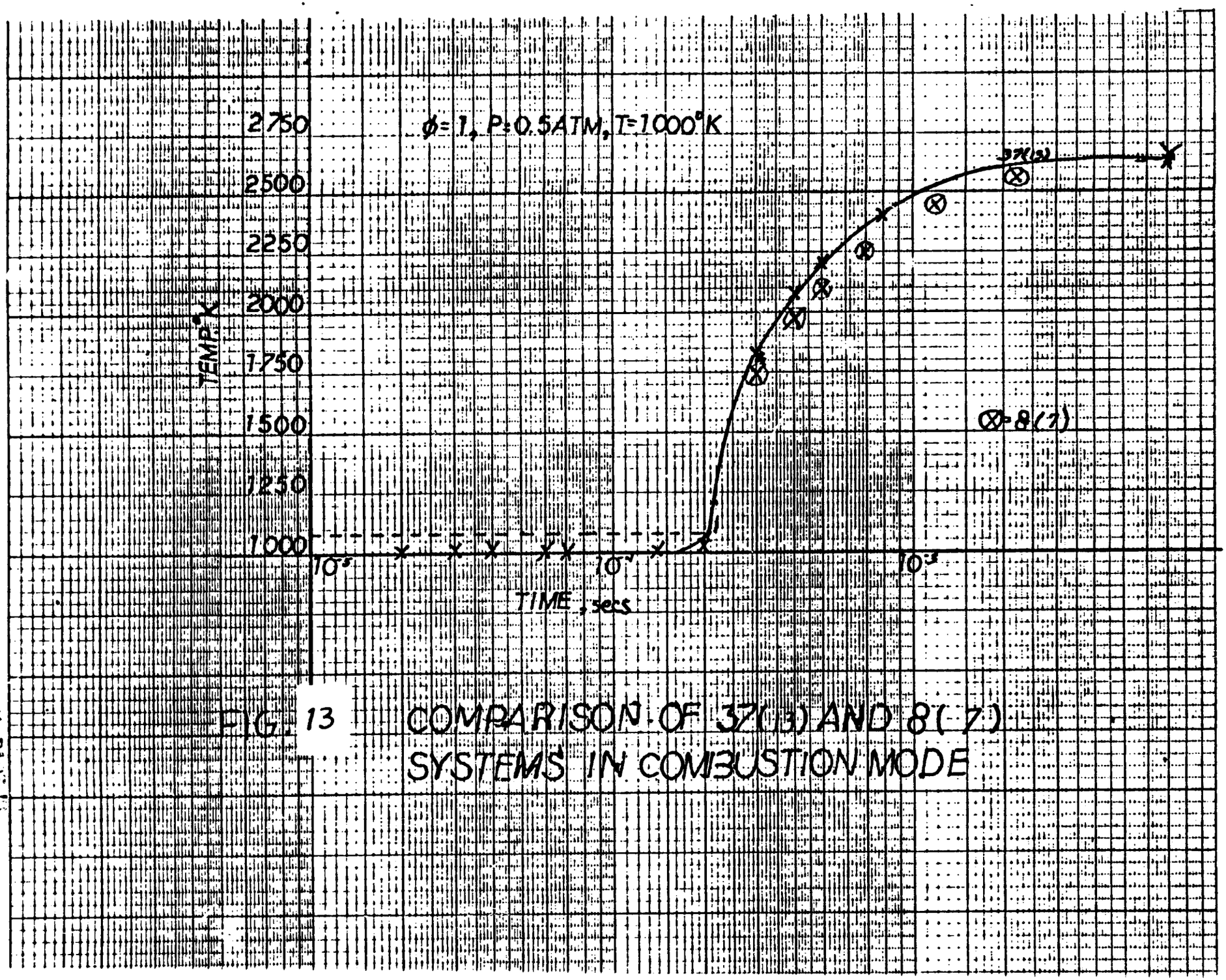

FIG. 13 COMPARISON OF 37(13) AND 8(7) SYSTEMS IN COMBUSTION MODE

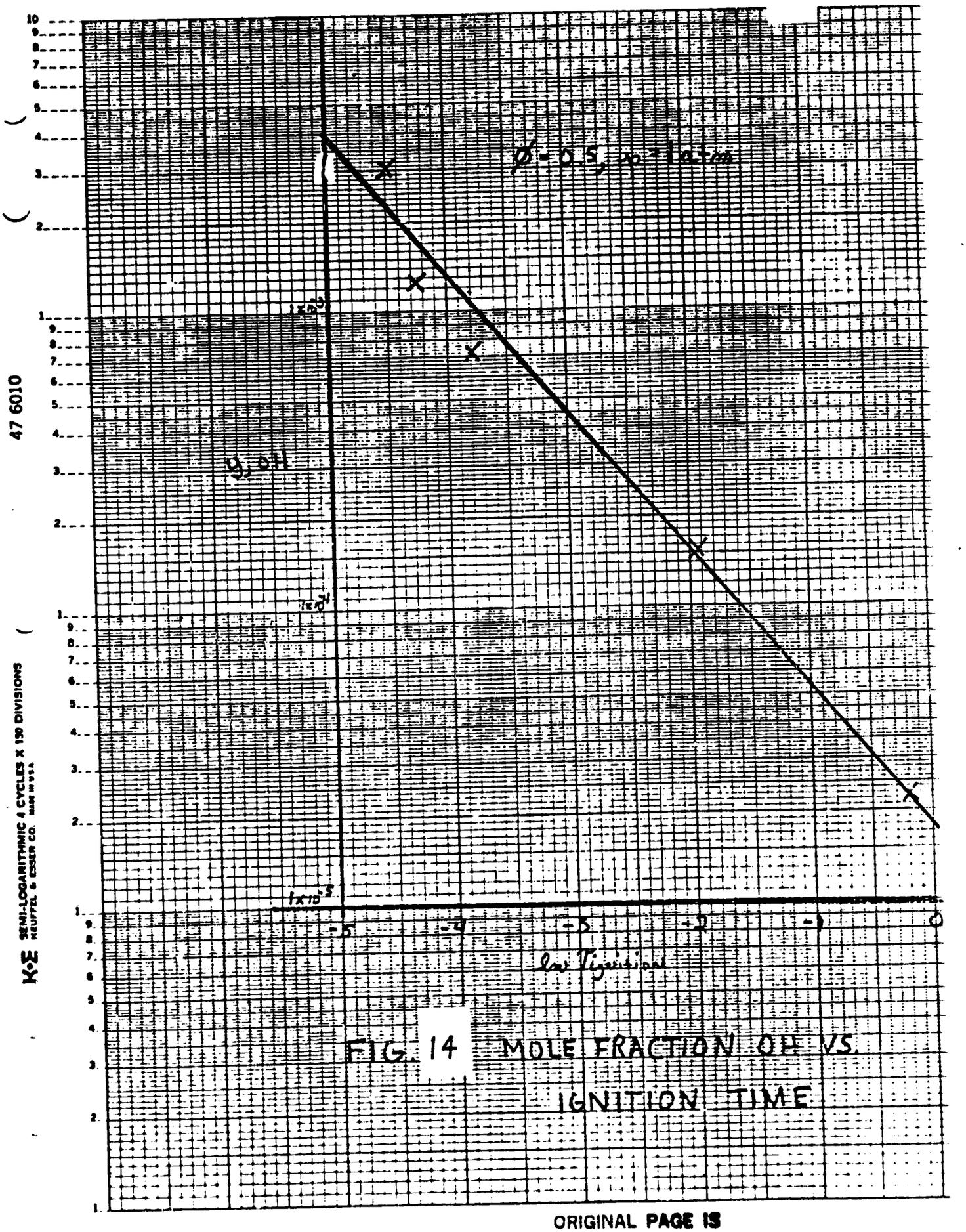

FIG. 14 MOLE FRACTION OH VS. IGNITION TIME

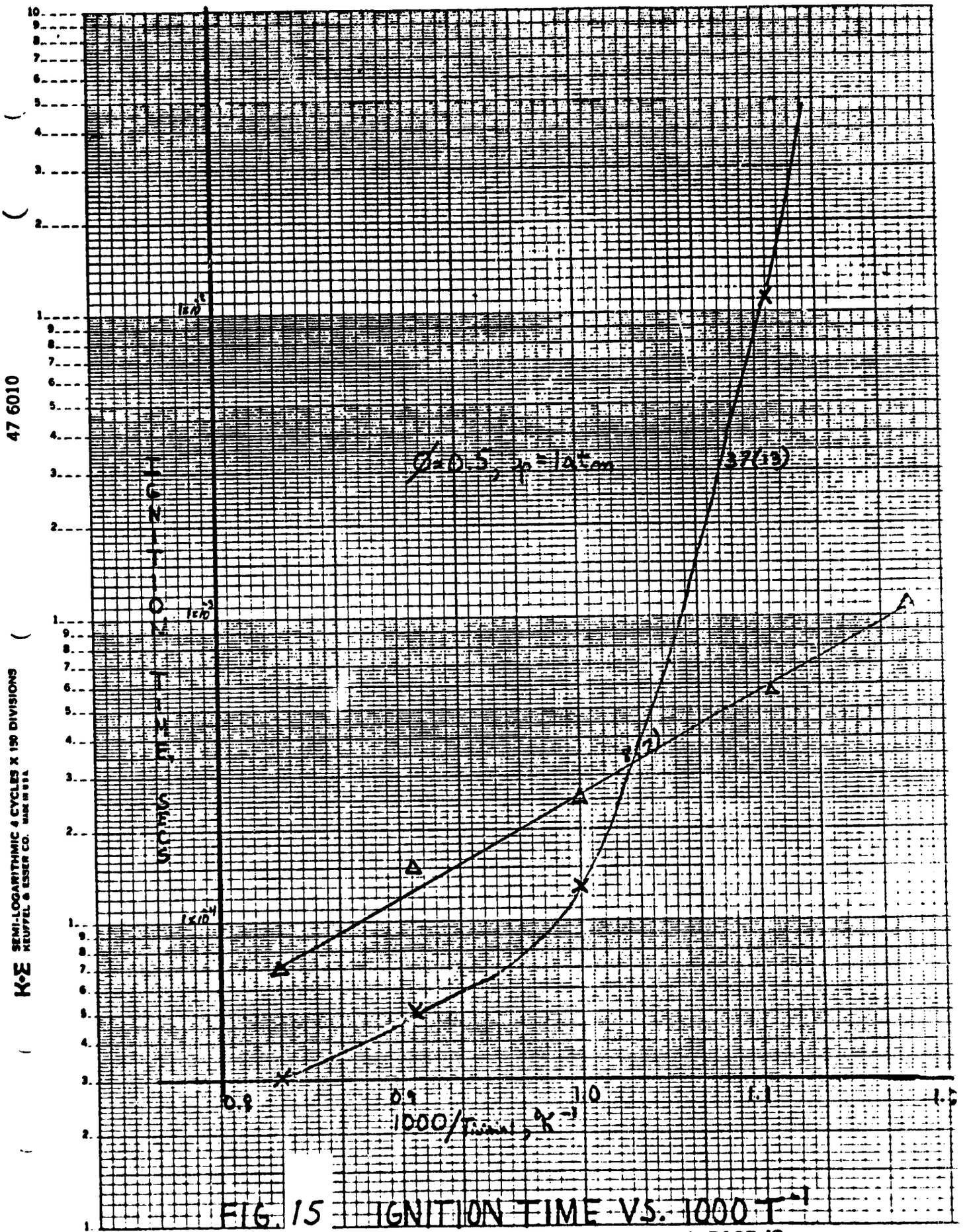

FIG. 15 IGNITION TIME V.S. 1000 T^{-1}

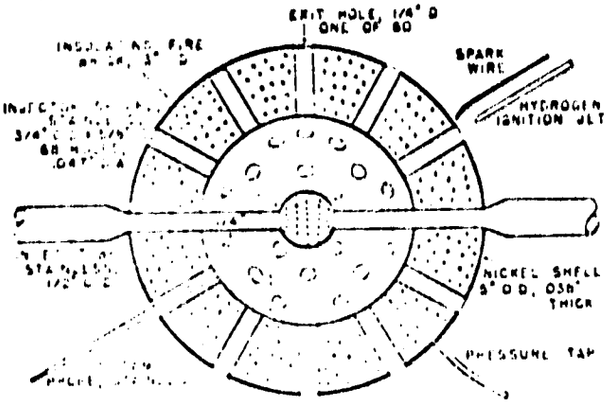

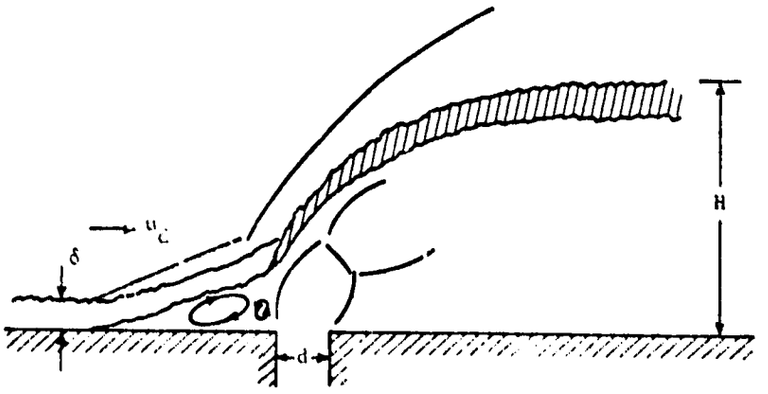

) Upstream recirculation model.

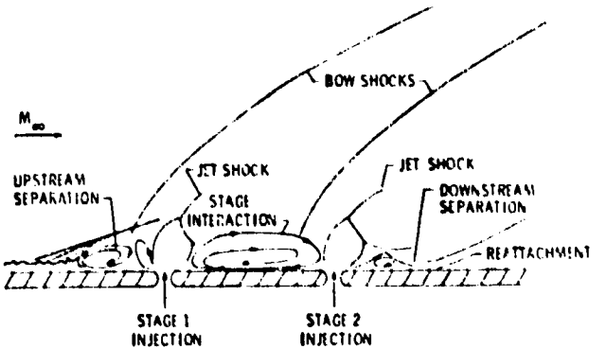

STAGED INJECTION FLOW FIELD SCHEMATIC

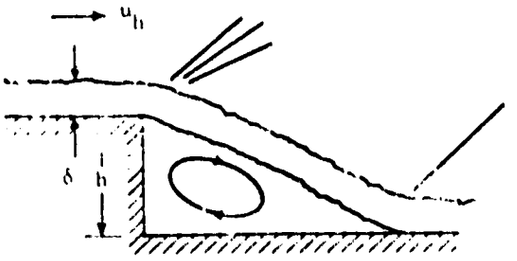

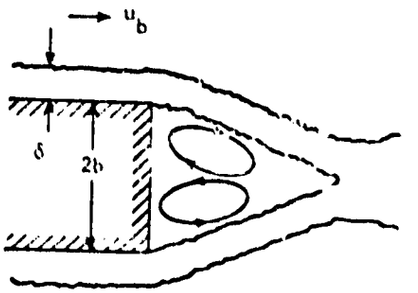

Step and base models.

FIG. 1C LABORATORY STIRRED REACTOR AND SCRAMJET RECIRCULATION REGIONS

FIG. 17. THE EFFECT OF INITIAL TEMPERATURE & FUEL SILANE CONCENTRATION ON RESIDENCE TIME AT BLOWOUT

STABLE FLAMES

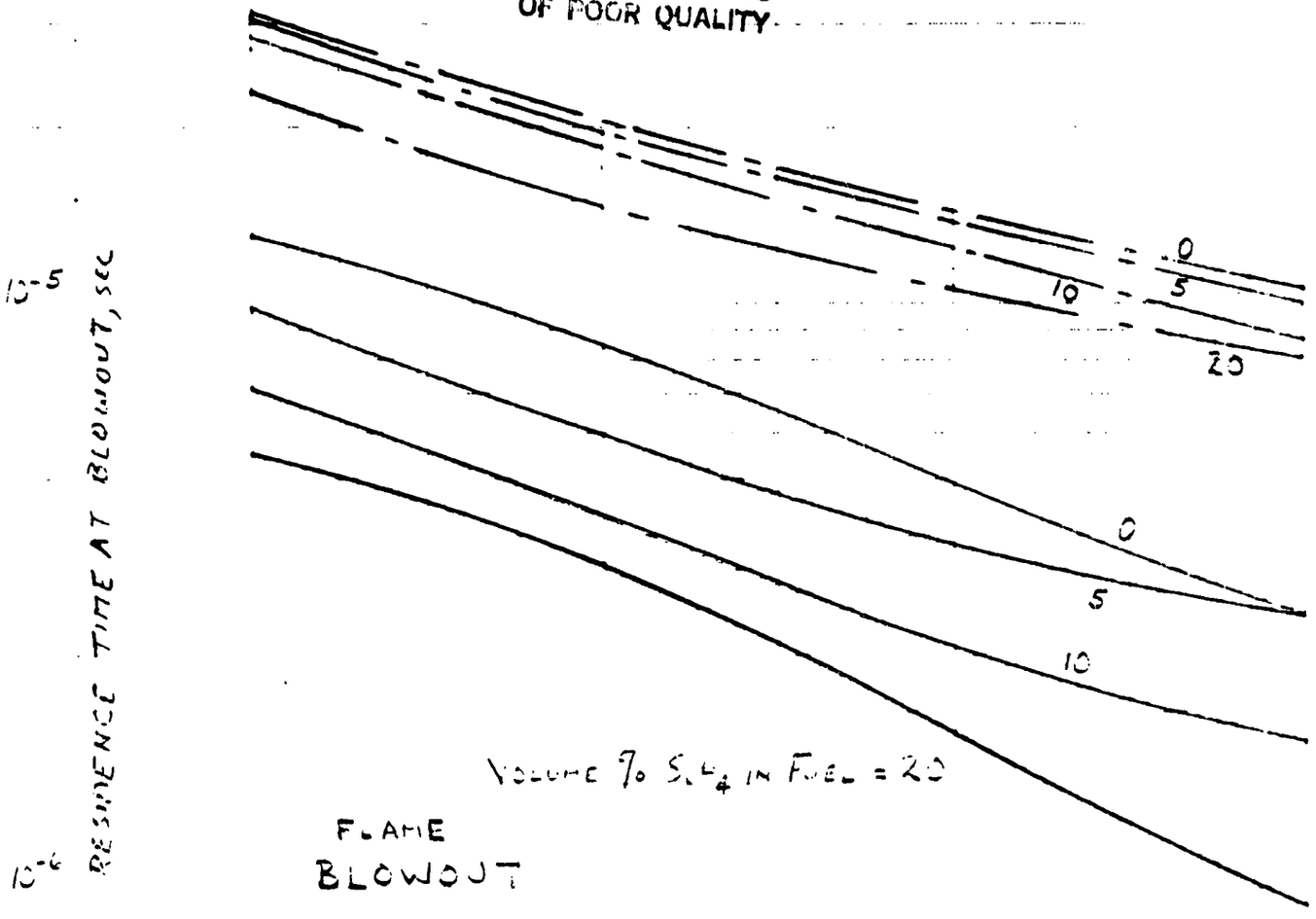

FIG. 18 THE EFFECT OF FUEL SILANE CONCENTRATION ON THE RESIDENCE TIME AT BLOWOUT

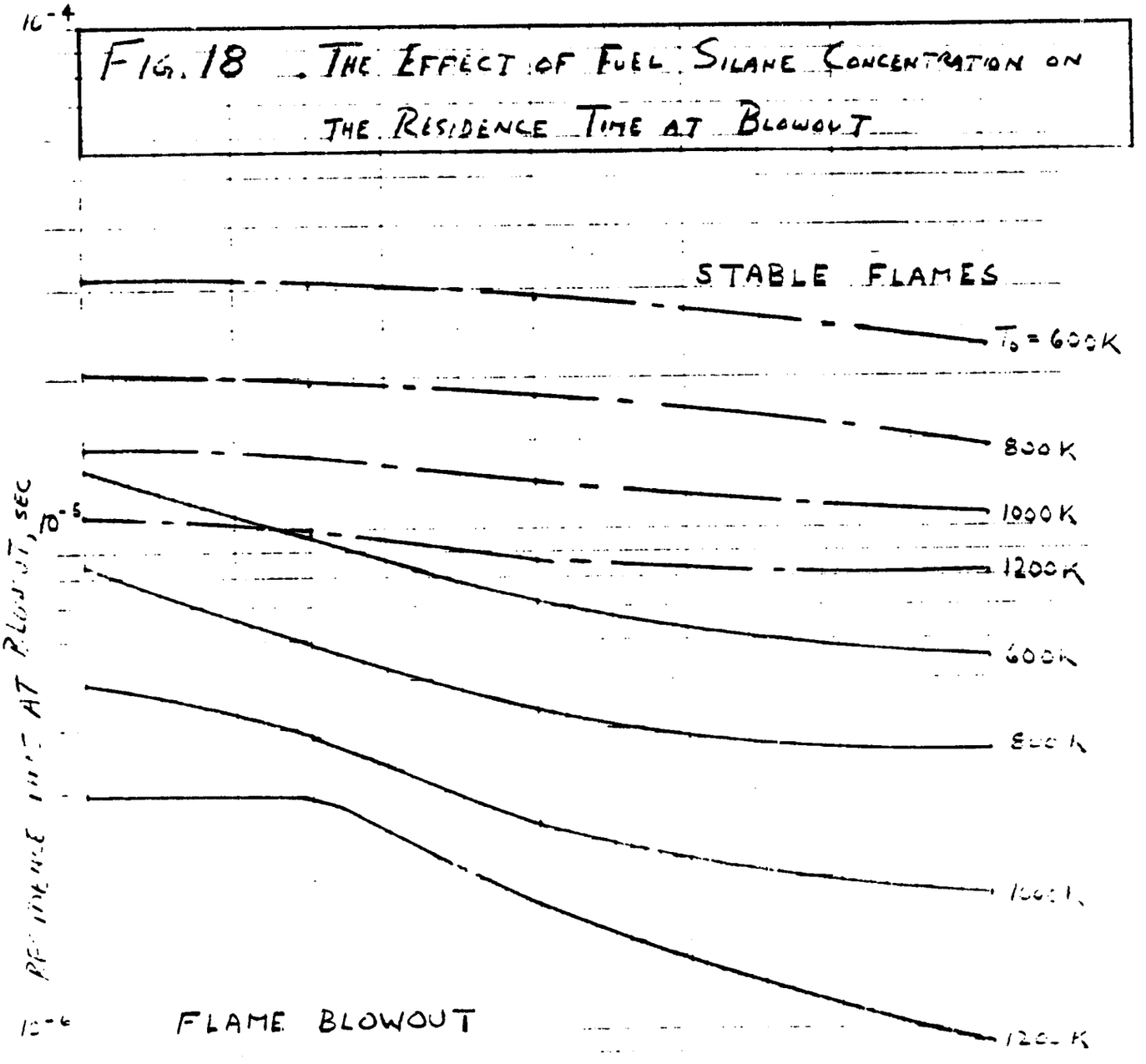

FIG. 19. THE EFFECT OF INITIAL TEMPERATURE AND PRESSURE ON THE RESIDENCE TIME AT BLOWOUT (SiH_4/H_2 FUEL)

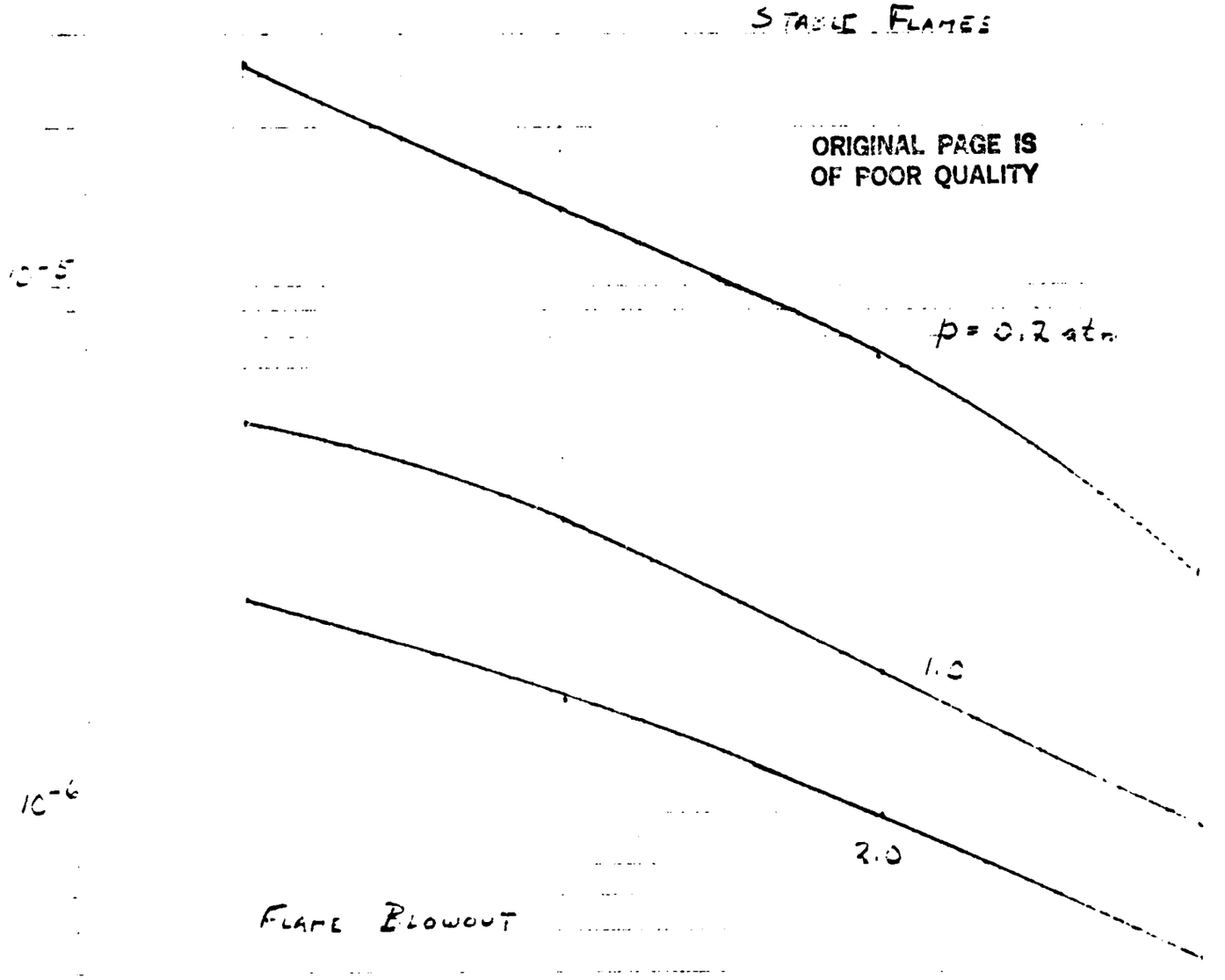

FIG. 20. THE EFFECT OF PRESSURE ON THE RESIDENCE TIME AT BLOWOUT (SiH_4/H_2 FUEL)

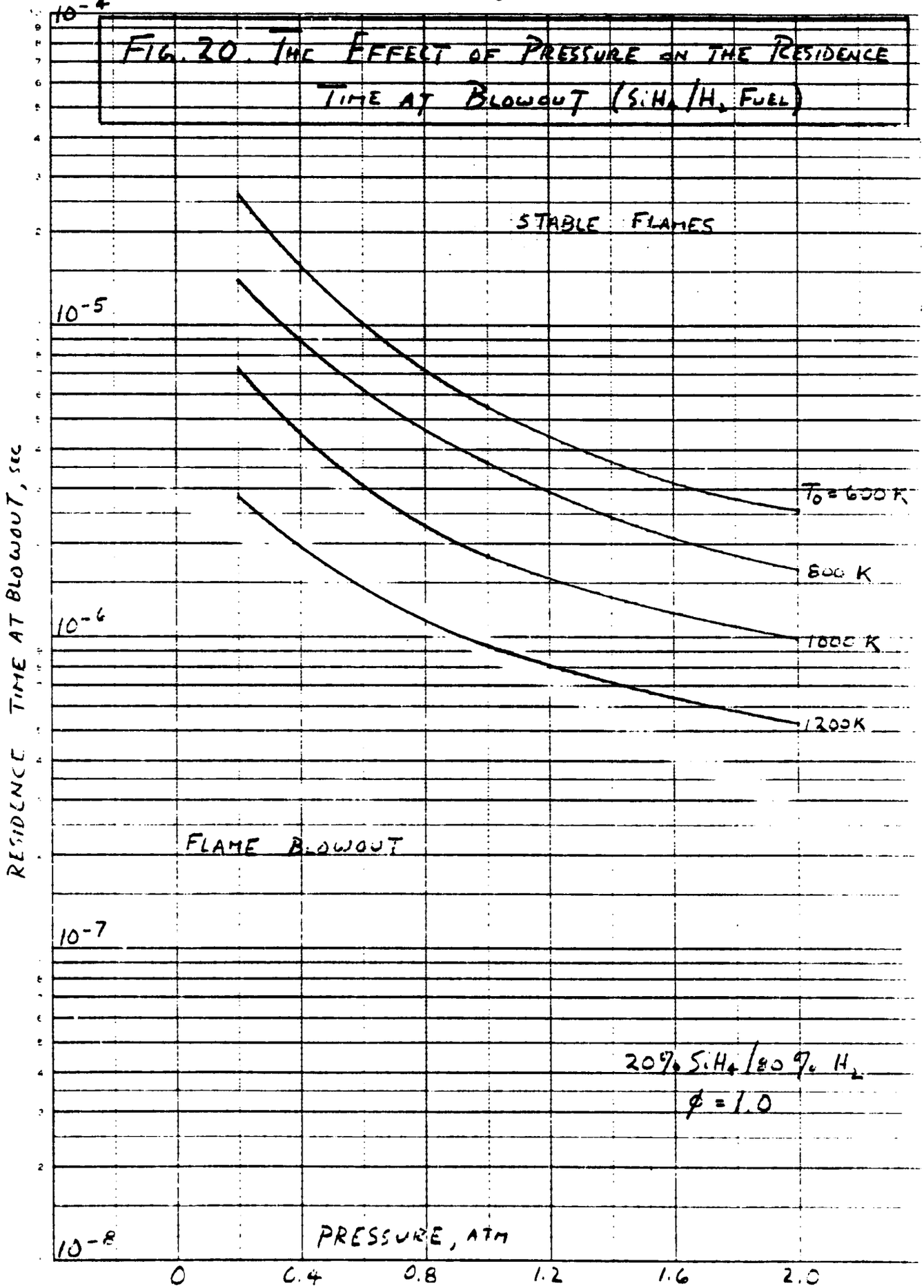

FIG. THE EFFECT OF INITIAL TEMPERATURE AND EQUIVALENCE RATIO ON THE RESIDENCE TIME AT BLOWOUT (SiH_4/H_2 FUEL)

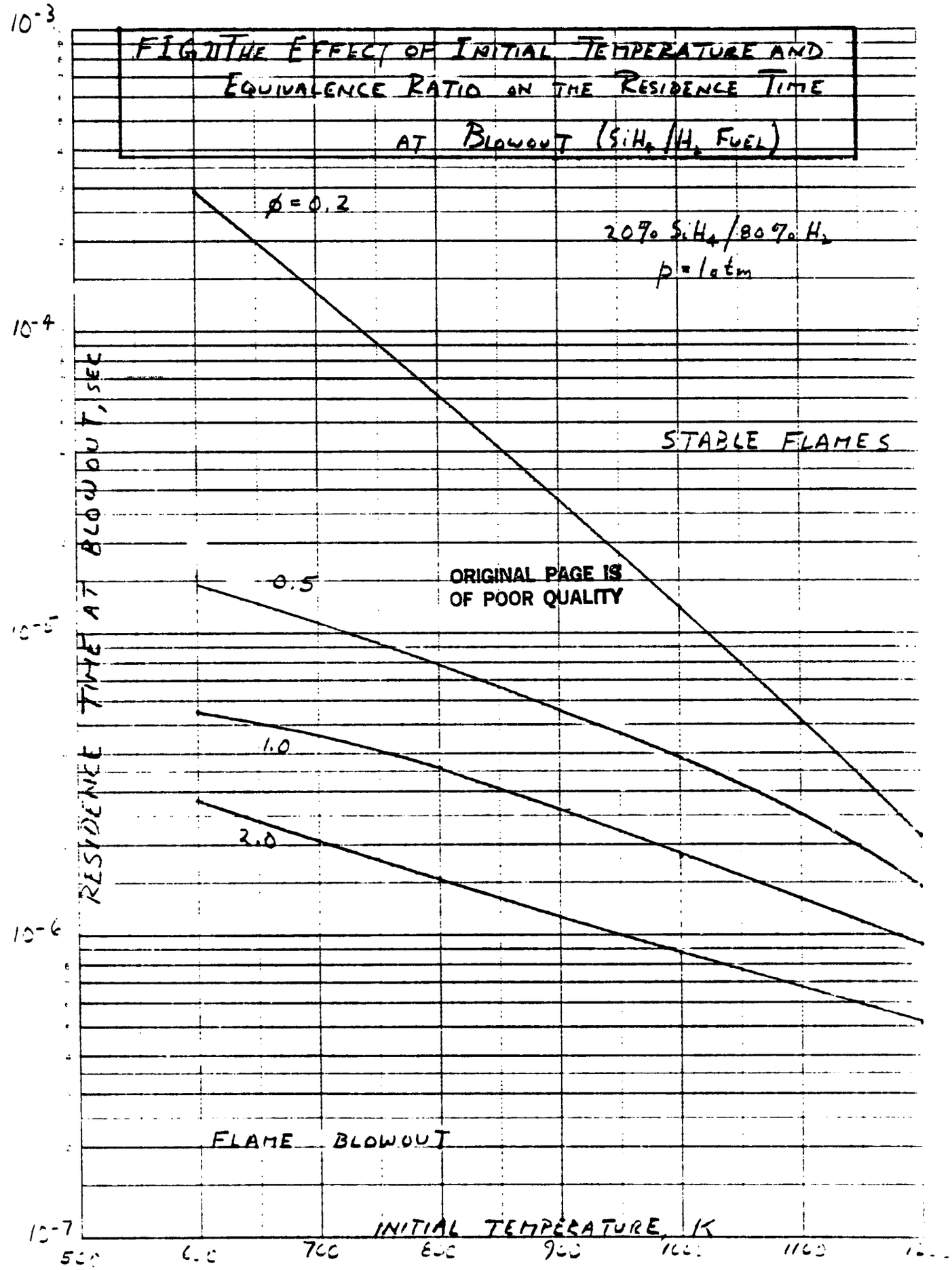

FIG. 22 . THE EFFECT OF EQUIVALENCE RATIO ON THE RESIDENCE TIME AT BLOWOUT (SiH_4/H_2 FUEL.

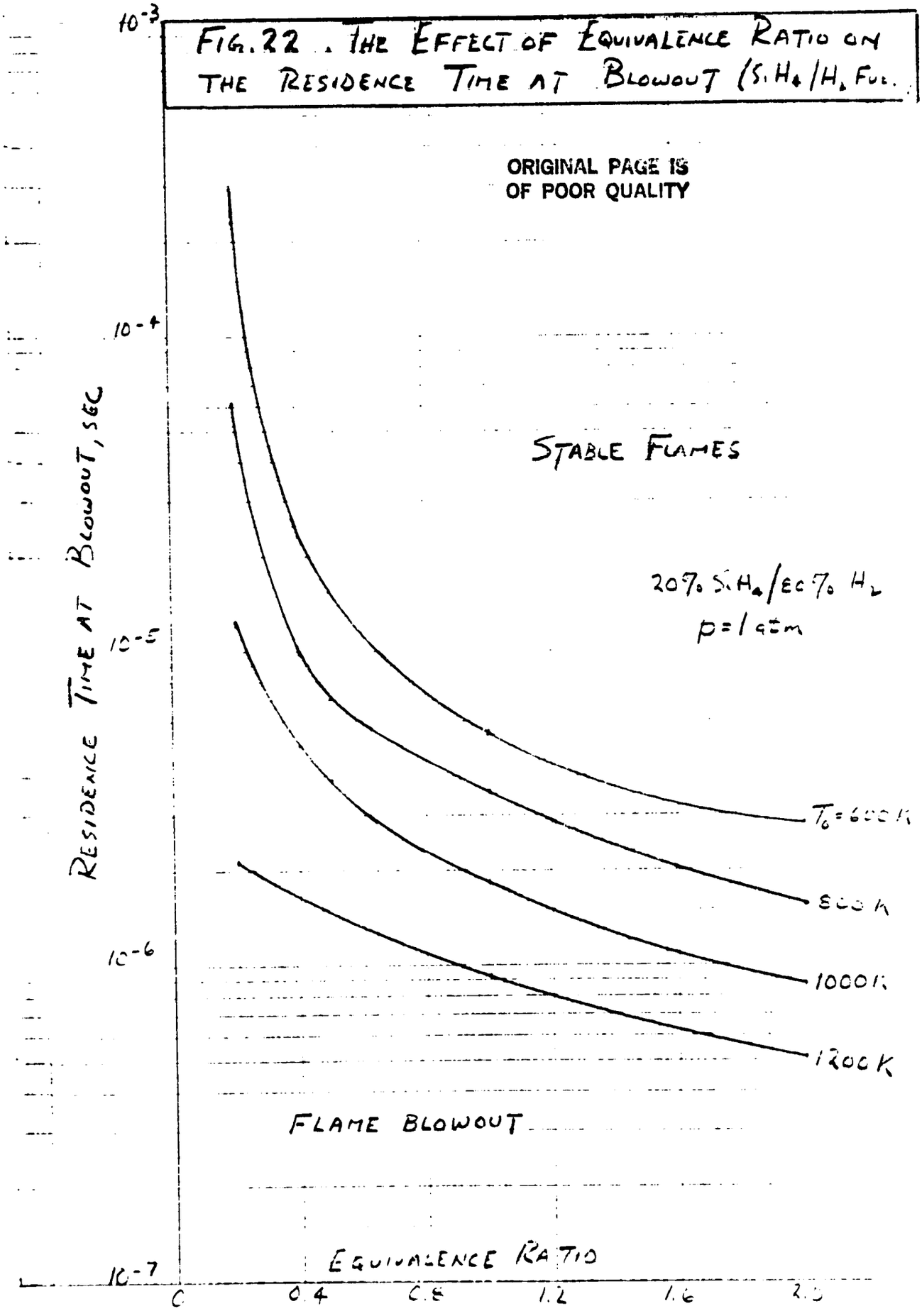

FIG. 23. BLOWOUT CORRELATIONS FOR SILANE-HYDROGEN FUELS

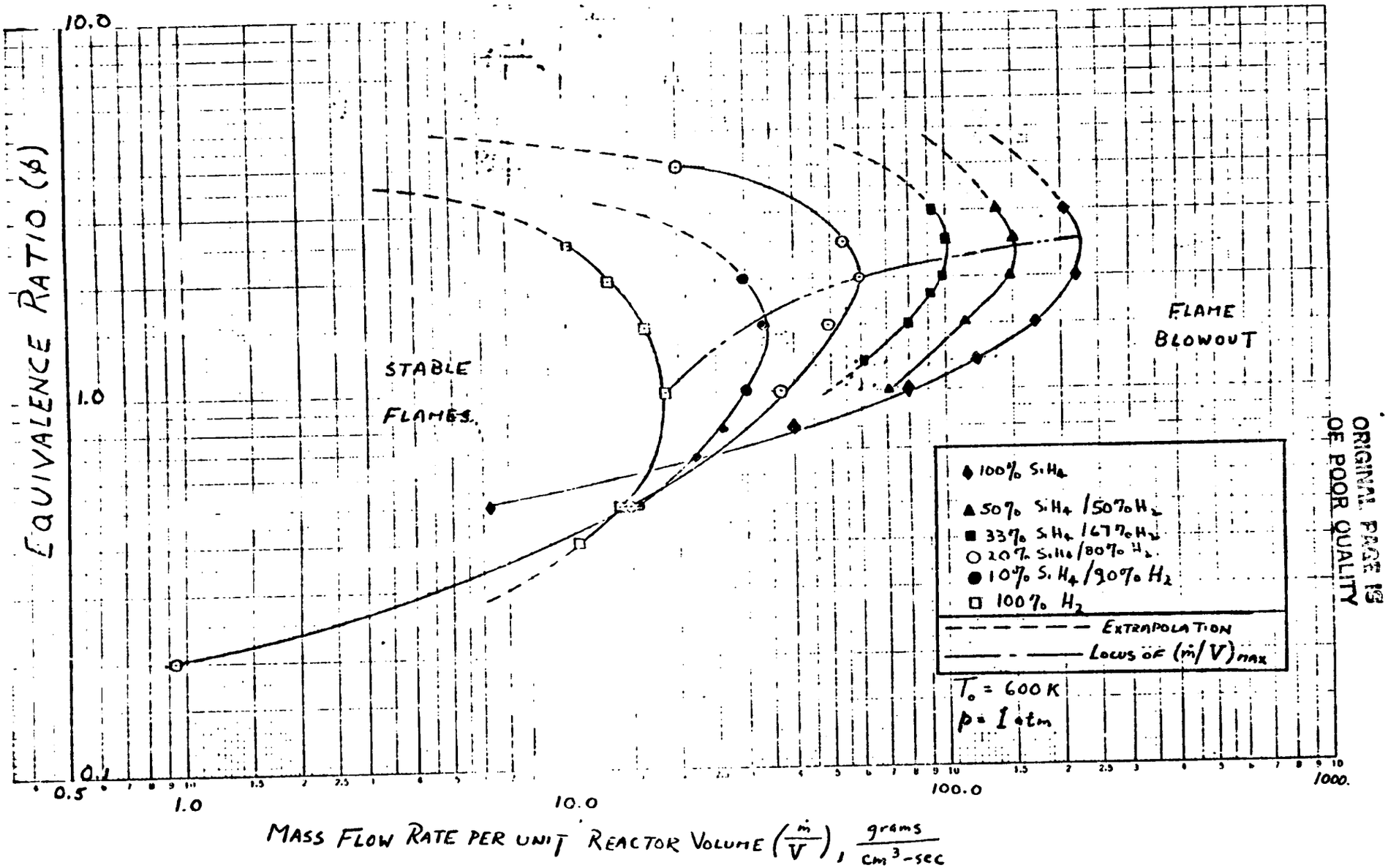

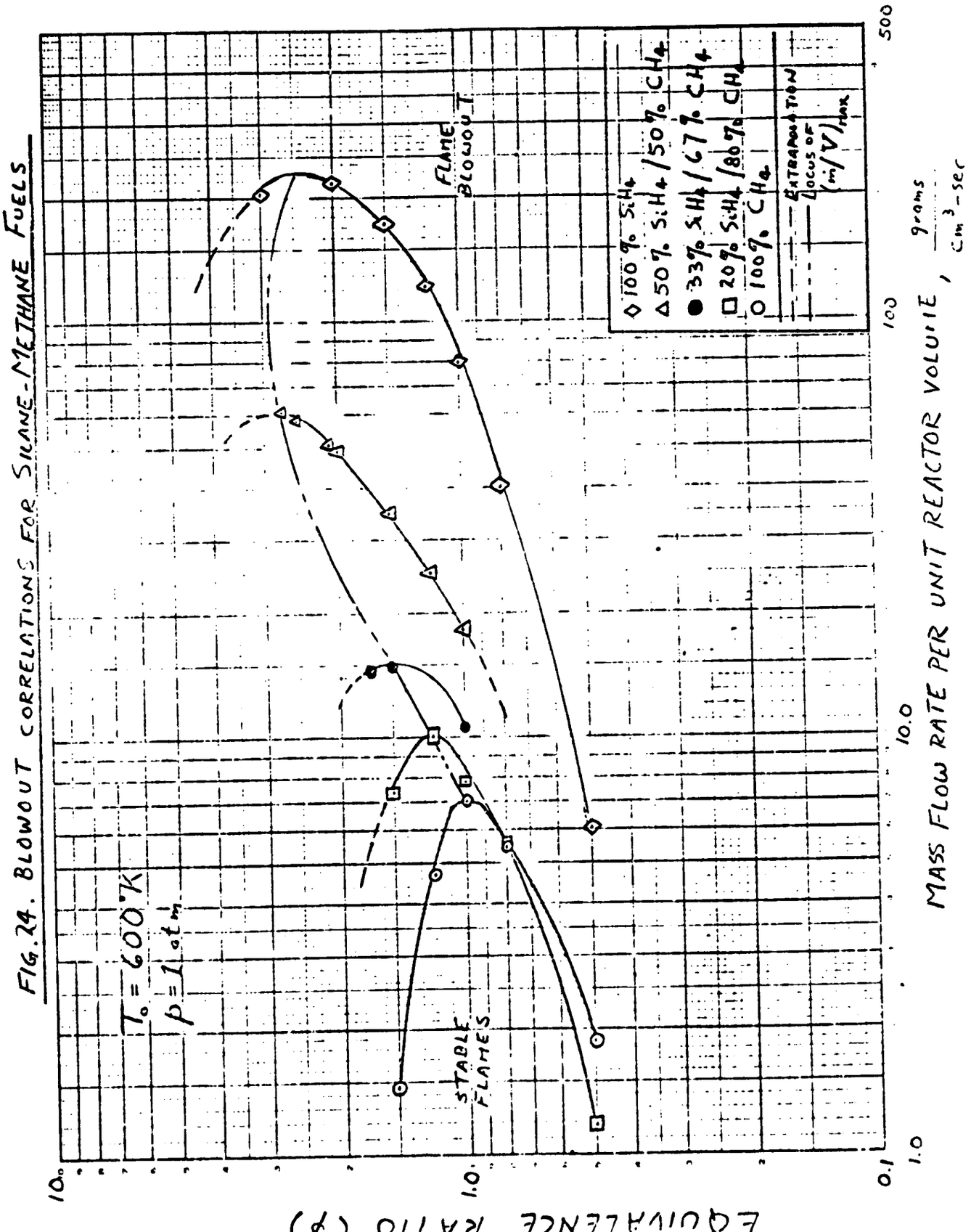

FIG. 25. BLOWOUT CORRELATIONS FOR SILANE-PROPANE FUELS

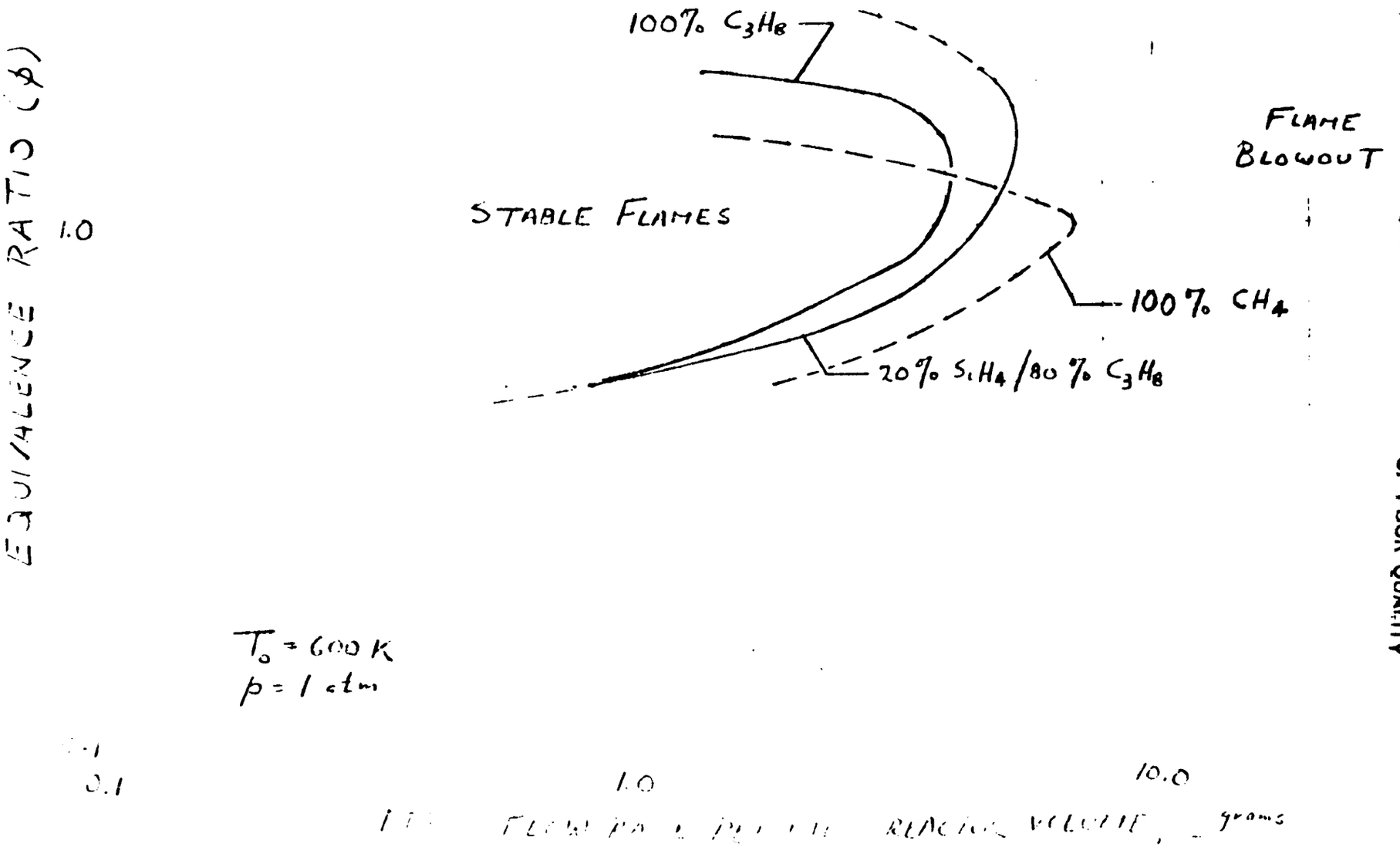

FIG. 26. THE EFFECT OF EQUIVALENCE RATIO ON THE MINIMUM RESIDENCE TIME REQUIRED FOR FLAME STABILIZATION

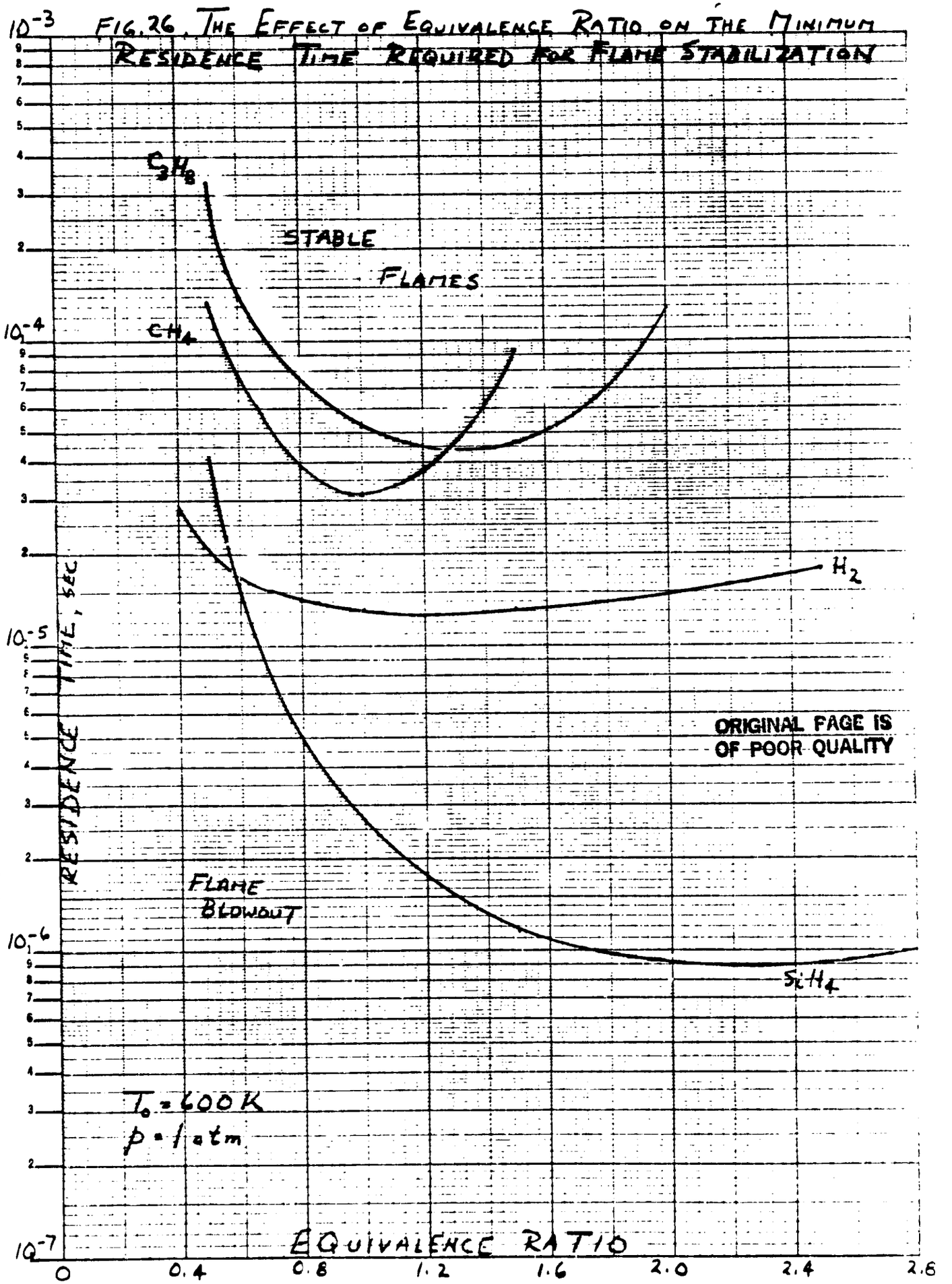

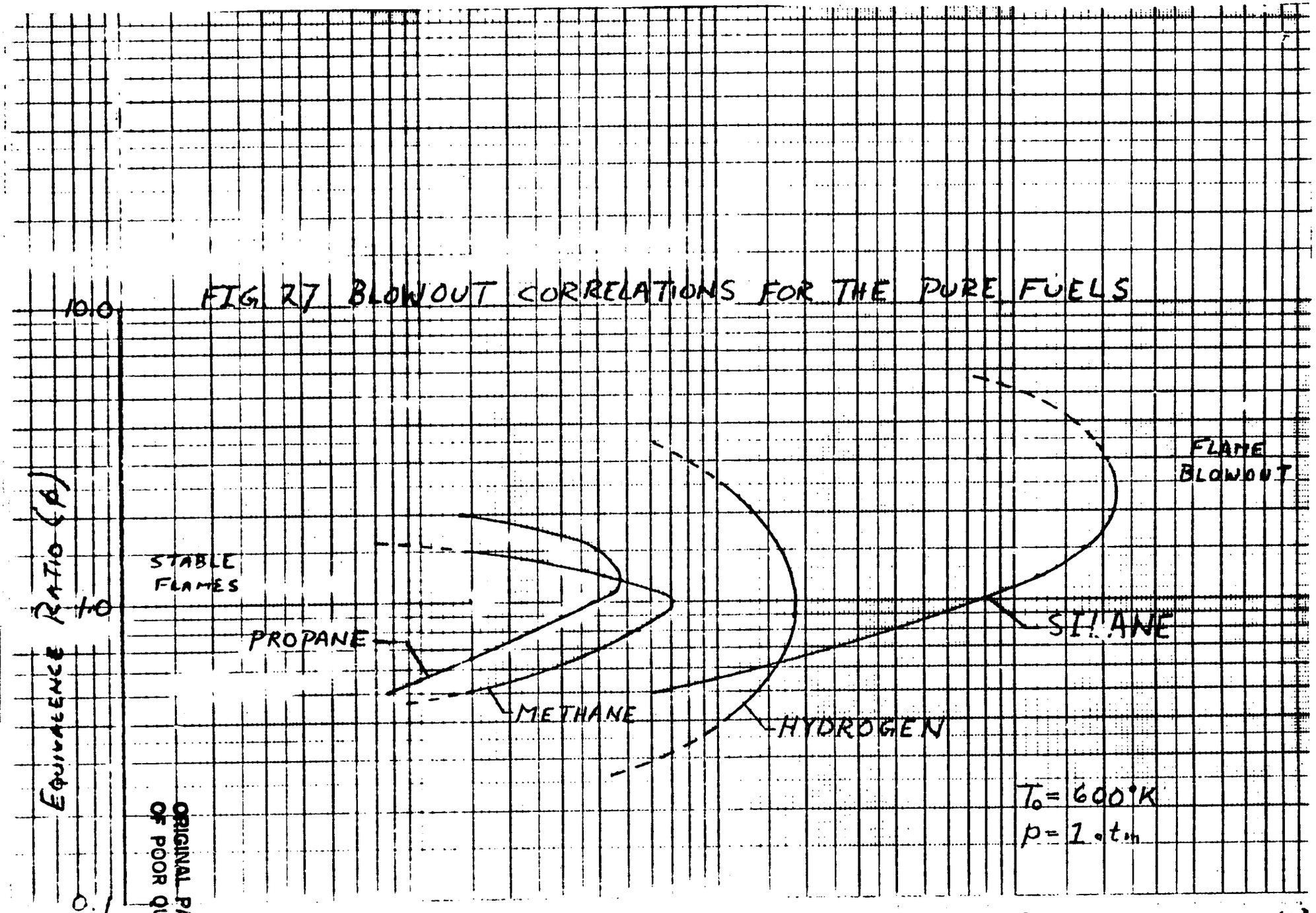

END

DATE

FILMED